

THESIS

IRON, HEPCIDIN, AND MICROCYTOSIS IN  
CANINE HEPATOCELLULAR CARCINOMA

Submitted by

Klaudia Zofia Polak

Department of Microbiology, Immunology, and Pathology

In partial fulfillment of the requirements

For the Degree of Master of Science

Colorado State University

Fort Collins, Colorado

Summer 2021

Master's Committee:

Advisor: Christine Olver

Anne Avery  
Kelly Santangelo  
Sarah Shropshire

Copyright by Klaudia Zofia Polak 2021

All Rights Reserved

## ABSTRACT

### IRON, HEPCIDIN, AND MICROCYTOSIS IN CANINE HEPATOCELLULAR CARCINOMA

Hepatocellular carcinoma (HCC) is the most common primary liver tumor found in dogs. There is evidence that iron dysregulation is associated with HCC pathogenesis in both humans and dogs. Anemia and thrombocytosis were common hematologic abnormalities detected in about half of dogs with massive HCC, and microcytosis was present in approximately 31% of dogs in one study. Additionally, humans with hereditary hemochromatosis have an increased risk of HCC. The liver is the major organ site for iron storage and metabolism containing numerous iron regulatory proteins which may play an important role in canine HCC.

Since microcytosis is associated with iron restricted erythropoiesis, our first objective was to determine whether neoplastic hepatocytes exhibit differential expression of iron regulatory genes as well as hepatic iron stores in normocytic versus microcytic HCC cases in an initial pilot study. Next, we aimed to quantify and compare expressions of a larger set of iron regulatory and human HCC-related genes among canine HCC tumor tissue, adjacent peritumoral liver tissue, non-specific reactive hepatitis liver tissue from non-HCC dogs, and normal liver tissue, as well as to quantify and compare estimated hepatic iron stores. We hypothesized that canine HCC tumor tissue exhibits iron overloading and higher expression of hepcidin and its upstream regulators (IL-6 and BMP6), which would promote intracellular iron availability for neoplastic hepatocyte proliferation. We also hypothesized that microcytic HCC cases would exhibit higher expression levels of hepcidin in tumor tissue compared to tumors from normocytic dogs. Additionally, we explored associations between clinical parameters and RNA levels of iron

regulatory genes as well as estimated hepatocellular iron stores in both HCC tumor and the adjacent, peritumoral tissues. We expected to find gene expression patterns in canine HCC tumor tissue related to abnormal regulation of iron metabolism and other pathways similar to what has been described in human malignancies.

Cases were selected from a database search for canine HCC and included if complete pre-operative blood work was available and there was adequate formalin-fixed paraffin-embedded (FFPE) tissue for RNA isolation for all cases. Hematologic and clinical parameters were recorded and used for correlation studies. All liver sections were reviewed by a board-certified veterinary anatomic pathologist. RNA was isolated from FFPE blocks and NanoString nCounter platform was used to quantify RNA counts for selected genes. Sections were stained with Perls Prussian Blue stain and hepatocytic iron stores were estimated using NIS-Elements software.

Contrary to our hypotheses, all canine HCC tumors had markedly decreased expression of hepcidin (HAMP) and depletion of hepatocellular iron stores. Other iron-related genes down-regulated in canine HCC tumor tissue included Tfr2 (an upstream regulator of hepcidin), STEAP2, LTF, HMOX1, CYBRD1 and SFXN5. Tumor tissue overexpressed Tfr1, STEAP3, and LCN2. No significant differences in RNA levels or iron stores were found between tumors of microcytic and normocytic HCC cases, but the adjacent peritumoral tissue was markedly iron loaded and exhibited negative correlation between hepcidin RNA levels and mean cell volume (MCV) as well as serum iron. Microcytic HCC cases were associated with noteworthy clinical findings such as increased ALT, lower HCT and serum iron, and histologically more poorly differentiated tumors. Differential expression of genes involved in Wnt signaling and ferroptosis was observed in canine HCC tumor versus the adjacent peritumoral liver tissue.

## ACKNOWLEDGMENTS

First and foremost, I would like to thank my brilliant and fearless advisor, Dr. Christine Olver, whose mentorship far surpassed her faculty duties. Your endless curiosity, optimism, and impressive expertise in numerous complex scientific divisions is an inspiration. Thank you for everything, including the millions of laughs.

I would also like to thank the faculty and members of the CSU Clinical Pathology Department and the Avery/Clinical Immunology Laboratory for excellent training and endless support during some of the hardest times of my life. Thank you for always challenging me to think deeper while providing a nourishing environment for both intellectual and personal growth.

In addition, I would like to thank my siblings (Olenka and Adam) and parents (Jolanta and Jerzy a.k.a. Tata) for pushing me to my full potential throughout my life and always believing in me. Especially Tata, my hero, who shaped me to be the person I am and worked hard his entire life so that we could follow our dreams. I did it, Tata!

Finally, I absolutely could not have completed this thesis work and residency program without the unwavering support, unconditional love, and constant encouragement from my husband and soulmate, Jack Daniel.

## TABLE OF CONTENTS

ABSTRACT.....	ii
ACKNOWLEDGMENTS.....	iv
Chapter 1 - Introduction.....	1
Background.....	1
Project Overview.....	7
Specific Aims.....	8
Chapter 2 - Pilot study.....	11
Pilot Study Materials and Methods.....	11
Pilot Study Results.....	15
Pilot Study Discussion.....	23
Chapter 3 - Expanded study.....	30
Expanded Study Materials and Methods.....	30
Expanded Study Results.....	33
Expanded Study Discussion.....	38
CONCLUSIONS.....	48
REFERENCES.....	50
APPENDICES.....	57
Supplemental Data.....	57

## CHAPTER 1: INTRODUCTION

### **BACKGROUND**

#### *Study significance*

Hepatocellular carcinoma (HCC) is the most common primary liver tumor found in both dogs and people<sup>1,2</sup>. In dogs, this neoplasm predominantly develops as a solitary mass<sup>2</sup>, which leads to a good prognosis if early resection is performed although incomplete surgical margins does not seemingly affect survival<sup>3,4</sup>. The solitary tumor morphology is described as massive, whereas the two other less common gross appearances of HCC are categorized as nodular and diffuse<sup>2</sup>. The majority of canine massive HCC are well-differentiated and only 0-7% of canine HCC-containing livers examined histologically were found to contain cirrhosis<sup>2,4</sup>, which is a marked contrast to human HCC. In humans, HCC predominantly arises from a background of cirrhosis and is highly associated with hepatitis B and C viral infections and alcohol abuse<sup>5</sup>. These predisposing conditions are nonexistent in the dog but in people generate a chronic inflammatory process in the liver that progresses to cirrhosis and ultimately HCC<sup>6</sup>. Interestingly, a small subset (up to 20%) of human HCC cases do occur in a non-cirrhotic liver<sup>6</sup>. Since the typical symptoms associated with cirrhosis do not occur, these HCC cases tend to be more insidious and not diagnosed until well into the advanced stages of disease thus making prognosis poor. More investigation into the etiology and pathogenesis of canine HCC is needed since most research surrounding human HCC is focused on cirrhosis and predisposing diseases that are not observed in our canine HCC patients. Additionally, finding similarities between canine HCC and the non-cirrhotic human HCC sub-type can highlight potential biomarkers and identify the dog as a useful animal model for this insidious cancer in people.

### *Hematologic abnormalities in canine hepatocellular carcinoma*

Studies investigating blood work changes in canine HCC repeatedly found that nonspecific increased activities of more than one liver enzyme occur in over 90% of dogs, with alkaline phosphatase (ALP) and alanine transaminase (ALT) activities being most frequently increased<sup>2,3,7</sup>. High serum activities of ALT and AST are indicators of poor prognosis in dogs with massive HCC<sup>3</sup>. One study reports that the mean levels of ALT, ALP, albumin and bilirubin were more often altered in liver neoplasia compared to degenerative non-neoplastic disease, indicating a more disturbed liver function in the malignant cases<sup>7</sup>.

Thrombocytosis is also a common finding in canine HCC and reported in about half of dogs with this hepatic neoplasm (46% of cases)<sup>2</sup>. Retrospective studies in dogs have concluded that in general thrombocytosis is predominantly attributed to a reactive process most commonly associated with inflammatory diseases and neoplasia, the top neoplastic category being carcinomas<sup>8,9</sup>. Thrombocytosis in people and rats has been strongly associated with iron deficiency as well, and although the exact mechanism remains unknown it appears that iron distribution favors megakaryocytic over erythrocytic precursors under iron deficient conditions<sup>10,11</sup>. Interestingly, abnormal iron status characterized by erythron parameters has been reported in a significant proportion of various histologic types of canine HCC, including anemia (approximately 50% of cases) and microcytosis (about 30% of cases)<sup>1,2,3,12</sup>. Microcytosis refers to abnormally small erythrocytes as measured by the mean cell volume (MCV). In a human study, people with HCC had a lower MCV and higher red cell distribution width (RDW) compared to healthy controls, although the actual percentage of people with microcytosis was not reported<sup>13</sup>.



### *Microcytosis and abnormal iron status*

When microcytosis is present on blood work in veterinary patients, the first differential considered is iron deficiency because this finding can indicate altered systemic iron metabolism that results in iron-restricted erythropoiesis (IRE). In general, IRE may result from: (1) absolute iron deficiency due to decreased absorption or loss of iron; or (2) functional iron deficiency caused by a decreased availability of iron in the face of normal or increased iron stores<sup>14</sup>.

Hemoglobin is synthesized in erythrocyte precursors within the bone marrow and its cytoplasmic concentration affects the maturation process of these early erythrocytes<sup>15</sup>. Once optimal hemoglobin concentration is reached, negative feedback occurs on DNA synthesis and stops erythrocyte division<sup>15</sup>. However, if overall hemoglobin concentrations are low due to decreased iron availability it is theorized that the erythrocytes undergo additional mitoses in order to reach optimal cytoplasmic hemoglobin concentrations resulting in smaller cells, also known as microcytes<sup>15</sup>. Defects in erythrocyte globin genes (hemoglobinopathies or thalassemias) or heme synthesis are best characterized in humans and often result in microcytic hypochromic anemia. Some of these conditions are also associated with concurrent tissue iron overload, particularly in the liver<sup>16,17</sup>.

Abnormal iron status characterized by hematologic parameters such as microcytosis with or without anemia, hypochromasia, low mean corpuscular hemoglobin concentration (MCHC) and low serum iron concentration is frequently described in dogs with portosystemic vascular anomalies<sup>18,19,20</sup>. Microcytosis in particular occurs in 33% up to 72% of dogs with congenital portosystemic shunts (PSS) and is significantly influenced by the concentration of serum iron<sup>19</sup>, but the exact mechanism still remains unknown. A few studies have also demonstrated increased iron tissue stores localized to the liver in PSS dogs<sup>18,19,21</sup>, and some showed low to normal iron

stores in the bone marrow<sup>22,23</sup>. Intriguingly, surgical correction of PSS in multiple reports resulted in reversal of abnormalities in iron status and most hematologic and biochemical indices<sup>19,20,22</sup>. Overall, these findings of abnormal hepatic iron stores and frequent microcytosis point to a functional iron deficiency or iron transport abnormality in the majority of untreated canine PSS cases<sup>22,23,24</sup>. In addition to iron deficiency and portosystemic shunts, microcytosis can commonly be seen in a significant proportion of healthy Akitas, Shiba Inus, Shar Peis, Chow Chows, and other Asian dog breeds<sup>25</sup>, but the mechanism is unknown and no overt evidence of abnormal body iron status is observed.

#### *Iron regulation and hepcidin*

Functional iron deficiency is seen in inflammatory and neoplastic conditions and is due in part to increased hepatocellular synthesis of a peptide hormone called hepcidin, considered to be the master regulator of iron<sup>26</sup>. Hepcidin functions to decrease intestinal absorption of iron and halt the release of body iron stores, which limits iron supply into the bloodstream. Systemic secretion of hepcidin by the liver is induced by the inflammatory cytokine interleukin 6 (IL-6) through the Jak/STAT3 (Janus kinase/signal transducer and activator of transcription protein 3) pathway and initiates the downregulation of ferroportin, the only known cellular exporter of iron<sup>27,28</sup>. Ferroportin is responsible for the export of iron from macrophages and enterocytes for delivery into the blood stream<sup>29</sup>. The degradation of ferroportin due to the binding of hepcidin results in decreased serum iron therefore cutting off iron availability for erythropoiesis. These systemic effects are highlighted in an early study in which mice that overexpressed hepcidin became hypoferremic and microcytic<sup>30</sup>. Transcriptional induction of hepcidin can also occur via BMP/SMAD (bone morphogenetic protein/small mothers against decapentaplegic) signaling

through sensing of a high iron load. The main up-stream regulator of hepcidin within this pathway is bone morphogenetic protein 6 (BMP6), which is locally produced in liver tissue by sinusoidal endothelial cells thus eliciting a paracrine effect on hepatic hepcidin synthesis<sup>13</sup>. Genetic defects within the BMP/SMAD pathway leads to hereditary hemochromatosis, a disorder of iron overload<sup>31</sup>.

### *Iron overload and cancer*

Iron is essential for the maintenance of life-sustaining cellular processes such as cellular respiration, oxygen sensing and transport, energy metabolism, and DNA synthesis and repair<sup>32</sup>. Due to its poor bioavailability and the severe consequences of deficiency, a major mechanism for iron excretion from the body does not exist and therefore can lead to serious consequences in cases of iron overload. Most of the excess iron reserves are stored in the liver whereas the remaining majority are used for erythropoiesis<sup>15,32</sup>. After uptake by the erythrocyte precursors, iron is incorporated into hemoglobin, a tetramer composed of globin proteins and iron-containing heme groups necessary for oxygen transport<sup>15</sup>. Despite its importance, iron is also involved in potentially harmful reactions such as the generation of reactive oxygen species which, when excessive, is linked to carcinogenesis through damage of various cellular components, particularly DNA<sup>32</sup>. Genome instability and increased mutability are major enabling characteristics of carcinogenesis that allow transformed cancer cells to acquire mechanisms for survival, proliferation, and dissemination<sup>33</sup>.

Multiple large epidemiological studies have discovered positive associations between increased body iron levels, determined using serum iron biomarkers, and development of various cancers<sup>34,35</sup>. Other cohort studies found that donating blood, which rids the body of iron through

loss of iron-containing hemoglobin, is associated with a lower cancer risk whereas receiving blood transfusions is associated with an increased cancer risk<sup>36,37,38</sup>. Iron is primarily acquired through the diet via intestinal absorption and studies led by the National Institutes of Health and the National Cancer Institute have found that people with diets largely consisting of processed or red meat, which has 10-fold higher concentrations of heme than white meat, had higher risk of esophageal, colorectal, lung, and liver cancers<sup>39,40</sup>. In particular, colorectal cancer has been extensively studied with regards to dietary iron intake and results repeatedly point to a positive association between red meat ingestion and incidence of carcinogenesis<sup>41,42,43</sup>. Collectively, the findings from all of these studies suggest that having increased body iron levels is associated with increased cancer risk.

Our interest in investigating systemic iron dysregulation in canine HCC grew even more after coming across studies showing a strong association between tissue iron overload in Hereditary Hemochromatosis (HH) patients and increased incidence of cancer. HH in humans is a disease of excessive absorption of iron into the bloodstream and deposition within tissues, particularly the liver, in the absence of iron deficiency<sup>44</sup>. HH is caused by mutations in genes that play an integral role in hepcidin iron sensing, which occurs through the interaction of iron-bound transferrin in the peripheral blood with the hepatocyte membrane-bound protein complex composed of BMPs and their receptors<sup>45</sup>, the co-receptor hemojuvelin (HJV), and other proteins such as the human homeostatic iron regulator protein (HFE) and second transferrin receptor (TfR2)<sup>44</sup>. HH patients have a significantly higher risk of hepatocellular carcinoma, about 20 to 200 times more than people without this disease, and are also more prone to colon, prostate, rectal, and breast cancers<sup>46,47</sup>. Research generated in the last decade has revealed dysfunction of iron metabolism regulation in a variety of carcinomas and hepcidin, the master regulator of iron

homeostasis, is often found at increased levels in the tumor tissue. Normal breast, prostate and intestinal cells have relatively low intracellular iron stores which promotes high ferroportin, low hepcidin, and low transferrin receptor 1 (TfR1) expression. Conversely neoplastic breast, prostate, and colorectal cancer cells gain the ability to synthesize extra-hepatic hepcidin resulting in measurably higher hepcidin expression compared to that of the normal surrounding parenchyma<sup>48,49,50</sup>. The effect of increased hepcidin production on intracellular iron metabolism is similar to what normally occurs when hepcidin is up-regulated in liver; aberrant tumor secretion of hepcidin causes ferroportin degradation which inhibits intracellular iron export and increases iron accumulation and availability within the rapidly dividing tumor cells<sup>49,50,51</sup>.

## **PROJECT OVERVIEW**

Due to the significant involvement of the liver in iron metabolism and previous reports of iron overload associated with cancer in humans, we aimed to investigate the expression of iron regulatory genes as well as the prevalence of iron loading in archival hepatocellular carcinoma (HCC) liver tissue from dogs. We hypothesized that canine HCC tumor tissue contains higher expression levels of hepcidin and its upstream regulators (IL-6 and BMP6), which would promote intracellular iron accumulation and availability for neoplastic hepatocyte proliferation, compared to the adjacent, peritumoral non-HCC tissue. We expected to find iron overloading in the tumor tissue secondary to hepcidin dysregulation. Since microcytosis is often associated with abnormal iron metabolism and sometimes hepatic iron overload in many species, we also hypothesized that canine HCC patients with concurrent microcytosis would exhibit higher expression levels of hepcidin in tumor tissue compared to tumors from normocytic dogs. This would support iron restricted erythropoiesis in the microcytic dogs given the known iron

sequestering effects of hepcidin. Additionally, we explored associations between clinical parameters and RNA levels of iron regulatory genes as well as estimated hepatic iron stores in both HCC tumor and the adjacent, peritumoral liver tissues.

The second part of our project is an expanded study to similarly investigate the differential expression of a larger set of genes related to iron metabolism as well as signaling pathways known to be involved in human HCC carcinogenesis in an effort to determine whether iron dysregulation exists in canine HCC and if similarities to human HCC are present. The focus shifts from microcytosis and other systemic clinical parameters to local HCC pathogenesis and hepatic iron regulatory genes. We hypothesized that canine HCC tumor tissue will exhibit abnormal iron metabolism and gene expression patterns similar to what has been described in human malignancies. This expanded study includes significantly more canine HCC cases and normal liver controls, with the addition of an inflamed, non-neoplastic liver tissue control group from dogs without HCC that histologically resembles the peritumoral non-HCC liver tissue found in most of our HCC cases.

## **SPECIFIC AIMS**

**Aim 1:** Determine whether there is a difference in iron storage or iron-related gene expression in canine HCC tumoral tissue compared to adjacent, peritumoral non-HCC tissue.

*Null Hypotheses:*

1. Canine HCC tumor tissue has higher expression levels of hepcidin and its upstream regulators IL-6 and BMP6, which would promote intracellular iron accumulation and availability for neoplastic hepatocyte proliferation, compared to adjacent, peritumoral non-HCC tissue.

2. Dogs diagnosed with HCC that also have concurrent microcytosis exhibit higher expression levels of hepcidin in tumor tissue compared to tumors from normocytic dogs, which would suggest iron restricted erythropoiesis in the microcytic dogs given the known iron sequestering effects of hepcidin.
3. Canine HCC tumor tissue is iron overloaded secondary to iron pathway dysregulation in transformed neoplastic hepatocytes.

*Objectives:*

1. Compare gene expressions of hepcidin (HAMP), IL-6, and BMP-6 in addition to six other iron regulatory proteins in archival specimens of canine HCC tumor and adjacent non-tumoral hepatic tissue using a direct digital counting method of RNA isolated from formalin-fixed and paraffin embedded tissues.
2. Investigate relationships among selected pre-operative clinical parameters, iron regulatory mRNA counts, and hepatic iron stores.
3. Quantify and compare hepatic iron stores among HCC tissues and normal liver controls using Perl's Prussian Blue staining and digital imaging measurement.

**Aim 2:** Gain insight on the pathogenesis of canine HCC and identify similarities to HCC in people.

*Null Hypotheses:*

1. Canine HCC tumor tissue is associated with iron metabolism dysregulation and exhibits a unique expression pattern of iron regulatory molecules and hepatic iron stores that differs in comparison to adjacent, peritumoral non-HCC tissue, normal liver controls, and inflamed, non-neoplastic liver tissue.

2. Canine HCC hepatic tissue exhibits a similar expression pattern of genes involved in the pathogenesis of human HCC, making the domestic dog a possible animal model for HCC.

*Objectives:*

1. Quantify and compare hepatic iron stores and expression of iron regulatory genes, as well as genes involved in other pathways that are reported to be significant in human HCC (total 89 genes), between tumoral and non-tumoral HCC tissue using an expanded set of archived canine HCC cases.

2. Compare results to normal liver controls and to an additional new group of inflamed, non-neoplastic liver tissues from dogs without HCC that histologically resemble the adjacent, non-tumoral tissue present in our HCC cases.



## CHAPTER 2: PILOT STUDY

### PILOT STUDY MATERIALS AND METHODS

#### *Case selection*

Cases with a diagnosis of “hepatocellular carcinoma” were found by searching the electronic medical records of canine patients seen between the years 2004 and 2014 at the Colorado State University (CSU) Veterinary Teaching Hospital. Permission for use of collected tissues was given at the time of patient admission. Cases were included in the study if patients had a complete blood count (CBC) and serum chemistry performed at the time of diagnosis, and adequate available tissue for RNA isolation in paraffin blocks from both HCC tumor and adjacent non-HCC, peritumoral liver tissue. The age at surgery was rounded to the nearest 0.5 years. CBCs were performed using EDTA anticoagulated blood (BD Vacutainer, Fisher Biosciences) on an Advia 120 automated hematology analyzer (Siemens Healthcare, Malvern, PA). Serum chemistries were performed on the Roche e911 (Roche, Basel, Switzerland). Serum iron measurement is included in the standard biochemical profile at CSU. Dogs were classified as “microcytic” if the MCV was less than or equal to 60 femtoliters (fL), and “normocytic” if the MCV was greater than or equal to 62 fL; the lower limit of the laboratory’s reference interval is 62 fL. Microcytic cases were selected first, and normocytic case controls (in approximately equal numbers to the microcytic cases) were chosen as the canine HCC cases with the closest date to the last microcytic case. Cases were excluded if they had co-morbidities that would affect iron metabolism, such as gastrointestinal bleeding or evidence of inflammation, or concurrent neoplasia other than HCC.

### *Histologic evaluation of liver sections*

Formalin fixed paraffin embedded (FFPE) blocks and corresponding hematoxylin and eosin-stained slides were collected from the Colorado State University Diagnostic Laboratory and Veterinary Teaching Hospital archives. For each HCC case, a board certified anatomic veterinary pathologist (PAS) confirmed the diagnosis of hepatocellular carcinoma and annotated the location of HCC tumor tissue and the adjacent, peritumoral non-HCC liver tissue. Histologic sections were also reviewed for concurrent idiopathic chronic hepatitis, hepatocellular necrosis, or other primary hepatocellular injury and excluded. Additionally, tumor differentiation was scored using a subjective system based on the degree of anisocytosis and anisokaryosis (mild, moderate, or severe) and architectural organization, and categorized as well differentiated (score = 1), moderately differentiated (score = 2), or poorly differentiated (score = 3).

### *Perl's Prussian blue staining and tissue iron estimation*

Perl's Prussian blue staining was performed on sections of paraffin embedded samples as previously described<sup>52</sup>, because there was not enough archived tissue available for both atomic absorption spectroscopy measurement of iron and RNA extraction. Four images (which included hepatocytes and Kupffers/macrophages) of randomly chosen sections were captured at 400x magnification for each case and combined into one composite tif file on Adobe Photoshop CC 2015 (Adobe Creative Cloud, <https://www.adobe.com/creativecloud.html>). The 4 images were chosen randomly by visualizing the HCC tumor or adjacent, peritumoral non-HCC areas at 40x objective, and then moving the section around blindly so that each 400x magnification field was chosen without subjective input. NIS Elements Software (Nikon, Melville, NY) was used to estimate iron quantity based on the total area of blue staining in pixels. Iron quantity in this

manuscript refers to the percent area (in pixels) of the composite images that was measured as positive (blue) for iron by the program.

### *RNA isolation and counting*

RNA was isolated from the archived FFPE blocks using a commercial kit (ReliaPrep™ FFPE Total RNA Miniprep System, Promega, Madison, WI). Using the corresponding and annotated histology slides as references, approximately 50 mg of tissue was excised from the HCC and non-HCC sections of each paraffin block for separate isolation of RNA. The samples were deparaffinized with mineral oil, followed by sample lysis, protein digestion, DNase treatment to remove DNA, and column isolation and elution of RNA. In cases where insufficient RNA was harvested (usually in non-HCC samples), the protocol was repeated but was altered by reducing the deparaffinization volume of mineral oil, and the final elution volume. RNA in each sample was quantified using spectrophotometry (Synergy H1, Biotek, Sinooski, VT). The RNA in each sample was diluted to a standard concentration of 40 µg/µL using RNase free water. RNA quality was evaluated with the High Sensitivity RNA assay on the Agilent 5200 Fragment Analyzer System with 33cm capillary array (Agilent, Santa Clara, CA) at the University of Arizona Genetics Core (University of Arizona, Tucson, AZ), where the digital counting was performed. RNA counting was performed using the NanoString nCounter gene expression system<sup>53,54</sup>. Briefly, the optimal amount of total RNA (150-400 ng) was hybridized with the custom codeset in an overnight incubation at 65°C, followed by processing on the NanoString nCounter FLEX Analysis System. The common names for the genes probed for in these experiments and their functions are listed in Table 1 (Table 1). GAPDH and beta actin were used as housekeeping genes. CD25 was chosen as a negative control gene that was expected to be low

and equal in both HCC tumor and adjacent non-HCC liver tissues. The RCC files provided by NanoString were analyzed using the nSolver software version 4.0. This software allows for raw count normalization to the expression of housekeeping genes and for background correction. For background correction, the means  $\pm$  2 SD of the negative controls were subtracted from the counts obtained for each gene.

### *Study design and statistical analyses*

Data were assessed for normality using the Anderson-Darling normality test. Non-parametric tests were used since most of the datasets were not normally distributed. Several analyses were performed with data from the dogs with HCC. The first analysis compared the HCC tumor and peritumoral non-HCC tissue values for RNA counts and iron in all dogs using a Wilcoxon matched-pairs signed rank test. The second analysis used a Spearman correlation to determine correlations between 1) RNA count number and selected erythrogram parameters and serum iron values from all dogs; 2) tissue iron quantity and the same laboratory values from all dogs; and 3) tissue iron quantity in HCC tumor and peritumoral non-HCC tissue RNA count number. The third analysis compared parameters between normocytic and microcytic groups using Mann-Whitney U tests (non-paired). This analysis included clinical parameters such as tumor differentiation score and selected hematologic and clinical chemistry values. It also included comparisons between HCC tumor tissue and the adjacent, peritumoral non-HCC liver tissue for RNA counts for each gene and estimated hepatic iron. All analyses were performed with commercial software (GraphPad Prism 8.2.1, San Diego, CA).

## PILOT STUDY RESULTS

### *Case selection results*

Out of 224 cases with HCC, 83 had a CBC at presentation (34%). Of these, 13 cases were microcytic. One Akita and one Shiba Inu mix were removed due to breed-associated microcytosis. One dog with a gastric foreign body was excluded due to the possibility of blood loss during surgical removal. Of the remaining 10 cases (12%), only 6 had paraffin blocks with enough tissue for RNA isolation from both HCC tumor and peritumoral non-HCC tissue. Seven normocytic HCC cases were identified, but sufficient RNA could only be isolated from 5 of the cases. The detailed clinical data for each individual dog are represented in Table 1.

### *RNA counts and iron in HCC tumor tissue compared with peritumoral non-HCC liver tissue*

Of the nine iron regulatory genes chosen for this analysis, only hepcidin and TfR1 counts were different between HCC tumor and peritumoral non-HCC liver tissues (Table 2). Hepcidin counts were significantly and markedly lower in the HCC tumor tissue; the mean count was 2.7% of that of peritumoral non-HCC tissue. On the other hand, the mean RNA counts of TfR1 was increased 3.04-fold in HCC tumor tissue compared to peritumoral non-HCC tissue. There were no significant differences in the RNA counts of BMP6, ferritin, ferroportin, HFE, IL-6, SFXN5, and SLC25a37 genes between HCC tumor and peritumoral non-HCC liver samples. Iron stores as estimated by Perl's Prussian Blue staining were 2.12-fold higher in peritumoral non-HCC tissue than in HCC tumor tissue. Comparisons of iron quantity, hepcidin counts and TfR1 counts between HCC tumor and peritumoral non-HCC liver tissues are shown graphically in Figure 1 (Figure 1).

*Correlation of gene expression with laboratory parameters and peritumoral non-HCC tissue iron load*

Hepcidin RNA counts in peritumoral non-HCC liver tissue showed statistically significant negative correlation with patient MCV ( $r = -0.76$ ,  $p = 0.009$ ) and serum iron ( $r = -0.75$ ,  $p = 0.025$ ) (Figure 2). Neither HGB nor MCHC showed significant relationships with hepcidin expression. Iron quantity in peritumoral non-HCC liver tissue was positively correlated with both hepcidin ( $r = 0.64$ ,  $p = 0.02$ ) and TfR1 RNA counts ( $r = 0.64$ ,  $p = 0.02$ ) in the same peritumoral non-HCC liver tissue (Figure 3).

*Microcytic and normocytic groups*

Summary clinical data, including tumor differentiation scores, are presented in Table 1 (Table 1). The median HCT and serum iron were significantly lower in microcytic dogs compared with normocytic dogs, while the serum alanine transaminase (ALT) was significantly higher. HCC from microcytic cases were more poorly differentiated based on our subjective histologic scoring. Of the nine iron regulatory genes evaluated, only tissue hepcidin RNA counts showed any significant expression differences between microcytic and normocytic dogs, and this difference was identified in the adjacent, peritumoral non-HCC tissue rather than the actual HCC tumor. Specifically, hepcidin counts were significantly higher in the adjacent, peritumoral non-HCC tissue of microcytic versus normocytic dogs. Estimated iron quantity was also significantly higher in the peritumoral non-HCC liver tissue of dogs with microcytosis compared to the peritumoral non-HCC liver tissue of normocytic dogs. These parameters, with each group divided into HCC tumor and peritumoral non-HCC liver tissue, are shown in Figure 4 (Figure 4). There was no difference in estimated iron quantity or counts of any regulatory genes between

HCC tumor tissue from microcytic or normocytic dogs. Representative photomicrographs of tissue from peritumoral non-HCC and HCC tumor tissues of microcytic or normocytic dogs, and a histologically unremarkable liver are shown in Figure 5 (Figure 5).

**Table 1.** Summary data for clinicopathologic variables for microcytic or normocytic dogs.

	Breed	Sex	Age at Surgery (Yrs)	HCT (%)	MCV (fL)	Serum Fe (uG/dL)	Serum ALT (IU/dL)	Tumor Differentiation	Tumor Differentiation Score
<b>NORMOCYTIC HCC CASES</b> (n=5)	Terrier mix	FS	11	49	70	145	120	Well	1
	Golden Retriever	MC	7	44	67	ND	246	Well	1
	Husky	MC	6.5	54	73	220	117	Well	1
	Golden Retriever	FS	13.5	45	75	124	43	Well	1
	Golden Retriever	FS	12	43	62	41	297	Moderate	2
<b>Mean±SD</b>	NA		10±3	47±4	69±5.1	132±74	165±104	NA	1.2±0.45
<b>MICROCYTIC HCC CASES</b> (n=6; MCV <62 fL)	Mix	MC	11	27	59	64	340	Moderate	2
	Mix	MC	12	41	59	138	825	Moderate	2
	Husky	FS	13.5	27	60	180	598	Moderate	2
	Mix	FS	10	50	59	ND	516	Poor	3
	Husky	FS	11.5	32	56	74	509	Moderate	2
	Norwegian Elkhound	FS	10	41	60	114	1297	Poor	3
<b>Mean±SD</b>	NA		11.3±1.3	36±10*	59±1.5*	114±48*	681±176	NA	2.3±0.52*

Abbreviations: HCT, hematocrit; MCV, mean cell volume; SeFe, serum iron; ALT, serum alanine aminotransferase.

\*Significantly different between microcytic and normocytic groups.



**Table 2.** RNA levels of nine iron-regulatory genes between all HCC tumor and adjacent non-HCC, peritumoral tissues (n = 11 of each tissue type).

<b>Gene</b>	<b>Function</b>	<b>Ratio*</b>	<b>P-value**</b>
Hepcidin	System iron regulator	0.03	0.0002
TfR1 (CD71)	Cellular iron acquisition	3.04	0.0479
BMP6	Hepcidin expression via BMP/SMAD pathway	0.51	0.4143
Ferritin	Intracellular iron storage	1.29	0.1831
Fpn	Cellular iron exporter	0.80	0.1716
HFE	Iron sensor	1.29	0.2146
Interleukin 6	Hepcidin expression via JAK/STAT pathway	0.98	0.2439
SFXN5	Mitochondrial iron storage	1.69	0.9097
SLC25a37	Divalent metal transport	1.04	0.7354

\*Values are presented as a ratio of the mean of HCC tumor RNA counts to the mean of peritumoral non-HCC RNA counts when total study sample data are combined irrespective of patient MCV. \*\*HCC tumor and peritumoral non-HCC RNA counts were compared using a Wilcoxon matched-pairs signed rank test

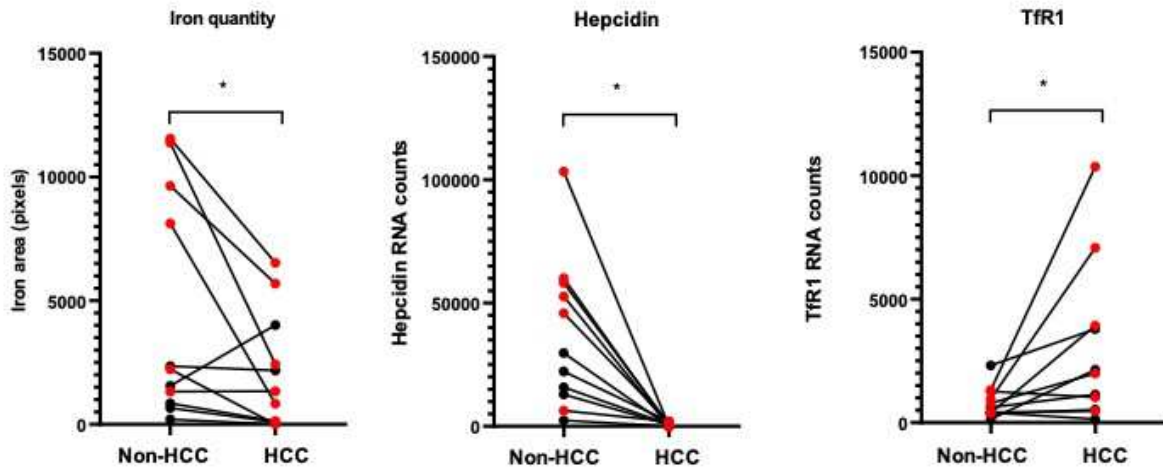


**Figure 1:** Iron quantity (left panel), hepcidin RNA counts (middle panel), and Tfr1 counts (right panel) in non-HCC tissue or HCC tissue. Iron and hepcidin were significantly higher and Tfr1 RNA significantly lower in non-HCC tissue compared with HCC liver tissue. Microcytic cases are represented by red symbols, and normocytic by black symbols. HCC = hepatocellular carcinoma. Asterisk indicates  $p < 0.05$ .

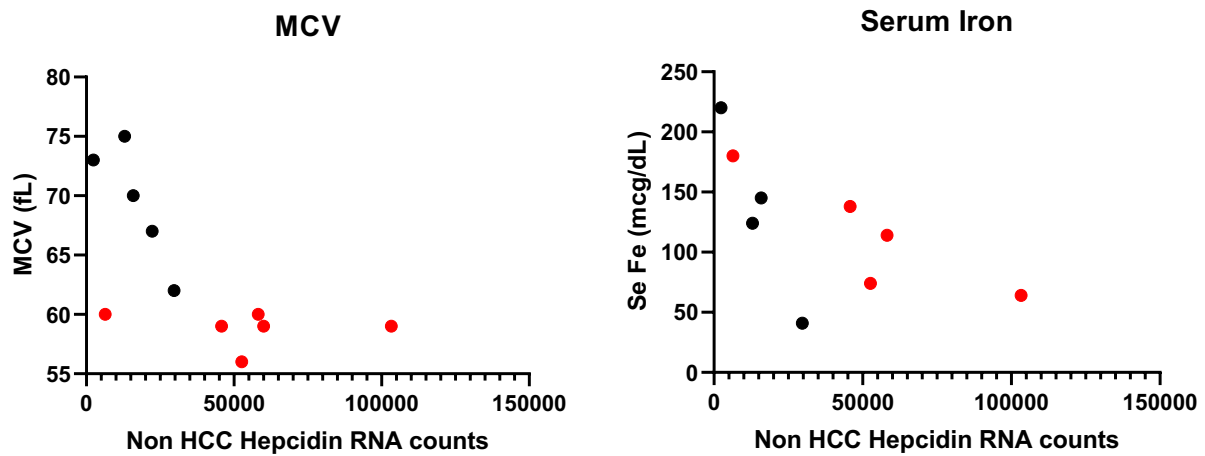


**Figure 2:** Scatterplots of MCV (left panel) or serum iron (right panel) and non-HCC hepcidin RNA counts. There was a negative correlation between non-HCC hepcidin RNA counts and both MCV ( $r = -0.76$ ,  $p = 0.0046$ ) and serum iron ( $r = -0.75$ ,  $p = 0.01$ ). HCC = hepatocellular carcinoma, MCV = mean cell volume. Red symbols represent microcytic cases, black symbols represent normocytic cases. Pre-operative serum iron values were not available for two of the cases.

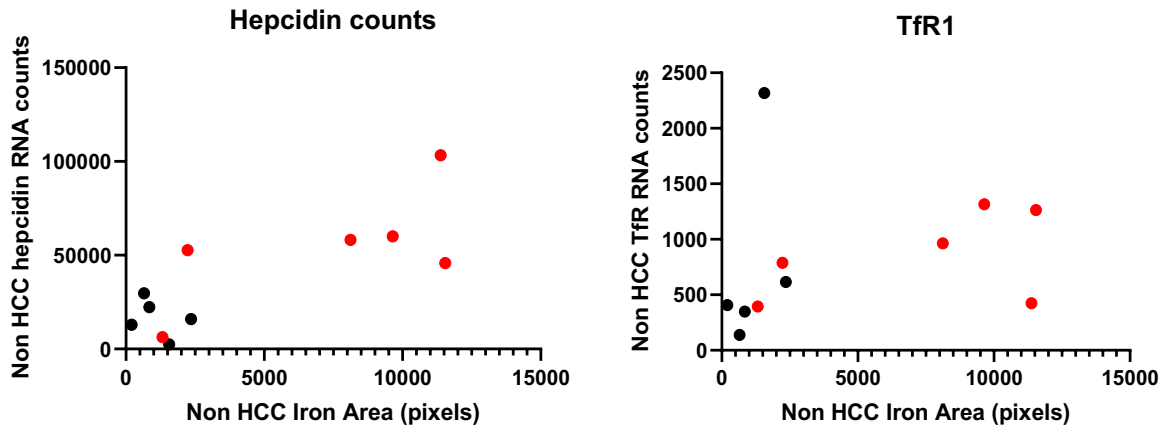


**Figure 3:** Scatterplots of hepcidin RNA counts (left panel) or TfR1 RNA counts (right panel) and non-HCC iron quantity. There was a positive correlation between non-HCC iron load and both hepcidin ( $r = 0.65$ ,  $p = 0.02$ ) and TfR1 ( $r = 0.64$ ,  $p = 0.02$ ). HCC = hepatocellular carcinoma. Red symbols represent microcytic cases, black symbols normocytic cases.

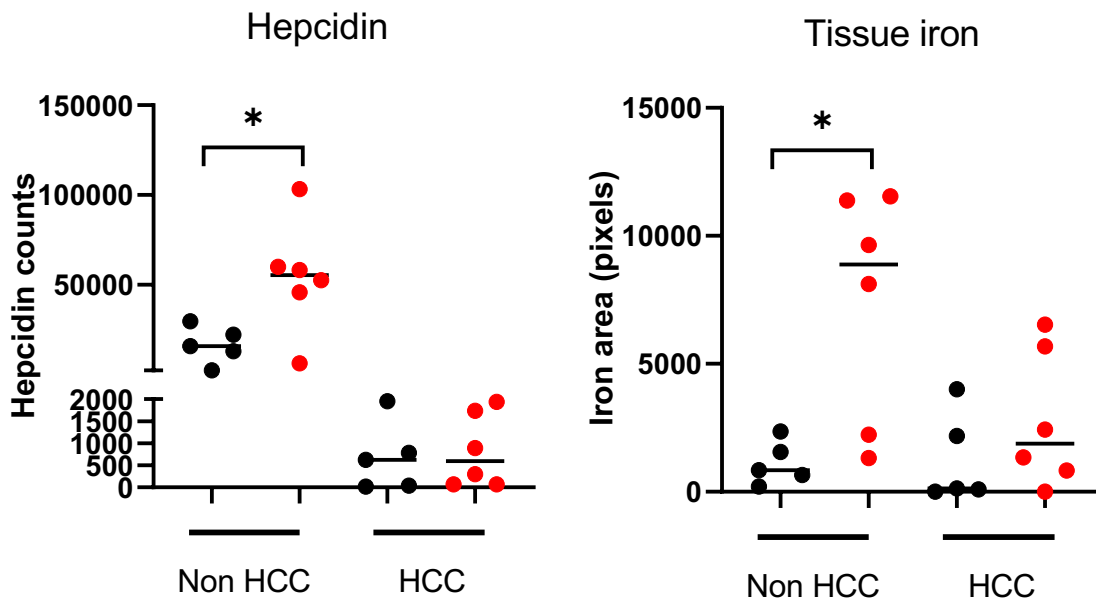


**Figure 4:** RNA counts for hepcidin (left panel) and iron quantity (right panel) as determined by digital area measurement of blue staining (Perl's Prussian Blue) shown for non-HCC or HCC liver tissue for normocytic groups (black symbols) and microcytic groups (red symbols). HCC = hepatocellular carcinoma. Statistically significant differences ( $p < 0.05$ ) are denoted with an asterisk\*.

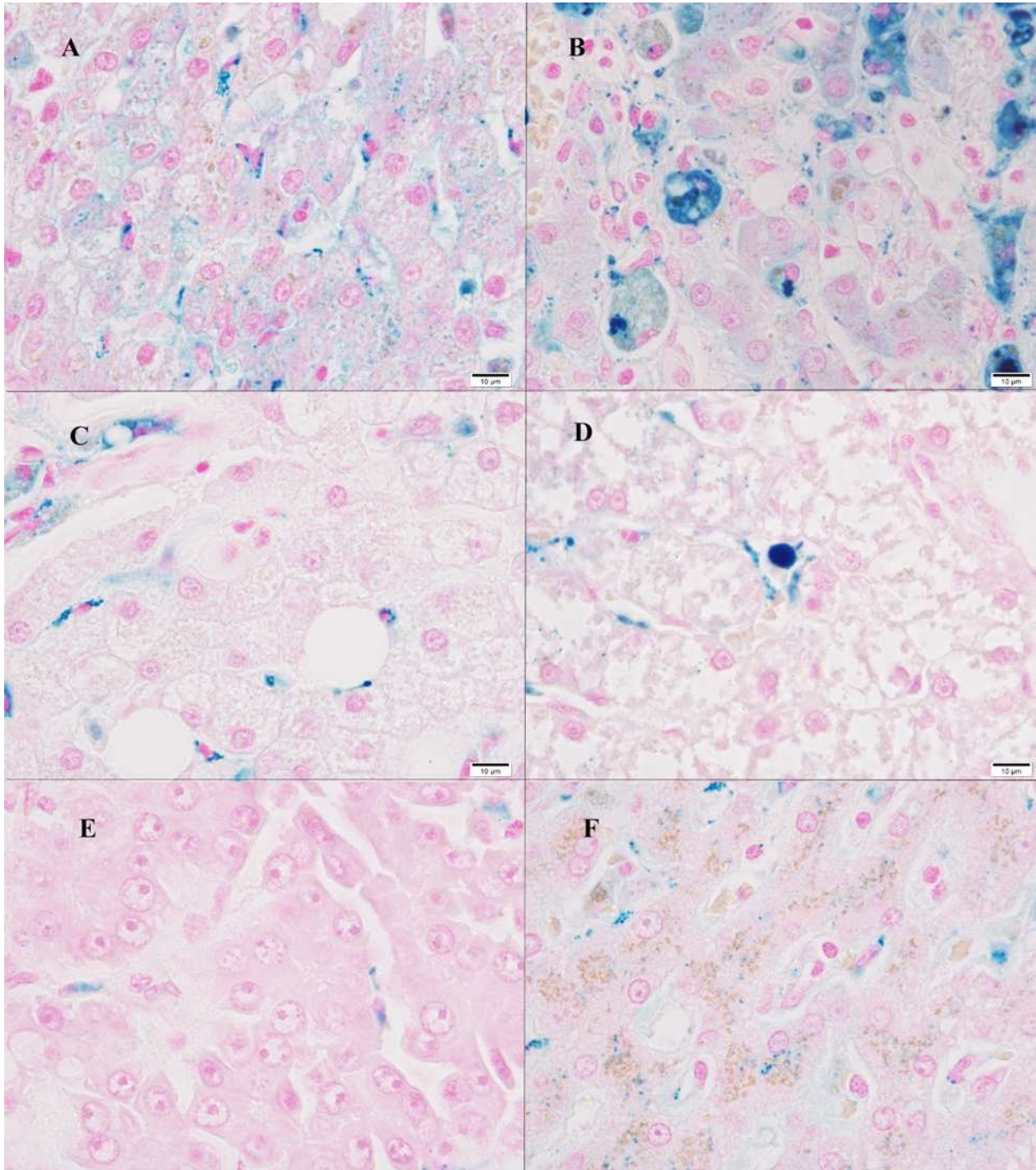


**Figure 5:** Representative photomicrographs of Perl's Prussian Blue stained histologic sections of non HCC tissue from microcytic dogs (panels A and B), non HCC liver tissue from normocytic dogs (panels C and D), HCC tissue from a microcytic dog (panel E), and tissue from a canine liver histologically assessed as unremarkable (panel F). HCC = hepatocellular carcinoma. Scale bars = 10µm, magnification = 400x.

## PILOT STUDY DISCUSSION

We performed a pilot study on archived canine HCC tumor and peritumoral non-HCC liver tissues to determine if the RNA of iron regulatory molecules is differentially expressed and/or quantitatively different between microcytic and normocytic cases. Additionally, we investigated whether differences in RNA expression and estimated iron quantity between canine HCC tumor and peritumoral non-HCC liver tissues are associated with microcytosis versus normocytosis. The most remarkable finding and contrary to our original hypothesis was that hepcidin expression was relatively low in all HCC tumor versus in the adjacent, peritumoral non-HCC liver tissue. Another unexpected finding was the differences in estimated iron stores in peritumoral non-HCC liver versus HCC tumor tissue, and the increased estimated iron in peritumoral non-HCC liver tissue of microcytic versus normocytic cases. Although we did not find differences in HCC tumor hepcidin RNA levels between microcytic and normocytic patients, we did find higher hepcidin RNA counts in the adjacent, peritumoral non-HCC liver tissue from microcytic patients when compared to normocytic patients. Furthermore, these microcytic HCC cases were associated with noteworthy clinical findings such as increased ALT, lower HCT and serum iron, and histologically more poorly-differentiated tumors.

Serum and cellular iron influence the expression of hepcidin in the liver. When serum and cells become iron overloaded, this stimulates hepcidin gene expression whereas on the contrary a deficiency in iron or increased erythropoiesis repress it<sup>55</sup>. In normal hepatic tissue, transferrin and non-transferrin bound iron is taken up by sinusoidal endothelial cells, which then release BMP6 in response to the increased iron load<sup>56</sup>. BMP6 is secreted in a paracrine fashion to act locally on hepatocytes via BMP receptors, along with the co-receptor HJV, and initiates transcription of hepcidin through the SMAD pathway<sup>13</sup>. This regulatory mechanism may explain

why higher peritumoral non-HCC liver iron stores in our study correlated with higher hepcidin expression. The low hepcidin expression in HCC tumor tissue compared with the adjacent, peritumoral non-HCC liver tissue in our study was surprising, but this phenomenon has been described previously in human HCC via a gene expression study<sup>57</sup>. The increased TfR1 levels in our HCC tumor versus the adjacent non-HCC tissue is an expected finding though, as this is common in various neoplastic cells when compared to their non-neoplastic counterparts<sup>32</sup>. We speculate that the accelerated iron utilization in neoplastic hepatocytes depletes their cellular iron stores quickly and results in increased TfR1 expression to promote iron uptake. The rapid iron utilization by neoplastic hepatocytes may also contribute to the decreased tumor hepcidin production. The depletion of iron may be sensed locally by sinusoidal endothelial cells and result in dampened paracrine BMP6 secretion within the tumor. Inhibition of BMP6 release disrupts the BMP/SMAD signaling pathway and thus could possibly contribute in some degree to decreased intratumor hepcidin production<sup>13</sup>. We did not see significant differences in BMP6 expression between HCC tumor and peritumoral non-HCC liver tissue, which could be due to a couple of reasons. Hepcidin regulation in canine HCC could be occurring via a different upstream molecule and pathway since both tissue types express similar levels of BMP6. The same theory could apply to the similar finding of no difference in the expression levels of IL-6, the other upstream hepcidin regulator examined in this study, in HCC tumor compared to peritumoral non-HCC liver tissue. Alternatively, differential expression of BMP6 could actually be occurring but below the lower limit of detection with our methods. Overall, the amount of BMP6 RNA counts measured was relatively very low throughout all samples. Since sinusoidal endothelial cells represent a small proportion of the total hepatic cellular population and consequently contribute to a small percentage of the total RNA harvested, it may be that our

analysis was not sensitive enough to demonstrate a difference in BMP6 RNA counts between HCC tumor and peritumoral non-HCC liver tissues.

We also speculate that the neoplastic hepatocytes may actually benefit from the effects of reduced tumor hepcidin levels locally on nearby iron-containing Kupffer cells. To briefly review, hepcidin binds to the iron exporter molecule ferroportin and results in its internalization and degradation. Reduced local hepcidin expression would presumably result in increased Kupffer cell ferroportin, which would allow for enhanced iron excretion and availability to the adjacent proliferating tumor cells. Considering our findings of increased iron loading in peritumoral non-HCC tissue and the absence of iron stores in HCC tumor tissue, it was surprising that ferroportin RNA counts were not different between the two tissue types. Since ferroportin expression is controlled post-transcriptionally<sup>58</sup>, we suspect that our RNA counts for ferroportin may not reflect the actual protein content, especially since hepcidin expression is so dramatically different between HCC tumor and peritumoral non-HCC hepatic tissues.

We found evidence of increased iron loading in the peritumoral non-HCC liver tissue of dogs with HCC. Although we used Perl's Prussian Blue staining as a surrogate for chemical measurement of iron, this finding is still intriguing. Review of the literature reveals a comparable pattern of differential iron staining in human HCC, which similarly shows a lack of iron accumulation in tumor tissue and excessive iron loading in peritumoral non-HCC liver tissue, along with a similar differential expression of iron regulatory genes between these tissue types<sup>57,59</sup>. This is an important finding in dogs since iron overloading in hepatocytes is associated with increased risk of HCC in humans. To re-emphasize, there is a 200-fold increased incidence of HCC in people with the genetic iron loading disorder hereditary hemochromatosis<sup>60</sup>, and dietary iron overload in humans also comes with a 24-fold increased risk of HCC<sup>61</sup>. When

examining the relationship between iron overload and liver disease, it is unclear which insult occurs first<sup>62</sup> or the specifics of subsequent HCC development. Iron induced carcinogenesis is thought to result from the DNA-damaging effects of reactive oxygen intermediates that result from the Fenton reaction involving free iron<sup>32</sup>, although iron also directly causes hepatocyte proliferation in rats<sup>63</sup>. Our data suggests that iron loading in the canine liver may be a risk factor for development of HCC since high amounts of iron were quantified in the peritumoral liver tissue of our HCC cases compared to normal liver controls. Increased liver iron content does occur in dogs, as is the case with chronic inflammatory liver disease<sup>64</sup>. Additionally, Harro et al. found that hepatic iron concentrations, measured with inductively coupled plasma mass spectrometry, were increased in non-HCC liver tissue compared with HCC tumor tissue which parallels our Prussian blue staining results<sup>65</sup>. The development of HCC as a sequela to iron loading has not been reported in dogs.

Several studies in humans have shown that different conditions that cause microcytic hypochromic anemia can be associated with iron overload in the body, the most common tissue being the liver<sup>16,17</sup>. Dogs with portosystemic shunts commonly have concurrent microcytosis<sup>66</sup>, and a few studies have demonstrated increased hepatic iron stores in these cases<sup>19,21</sup>. The findings in these previous reports combined with our observations of higher hepatic iron loading in adjacent peritumoral liver tissue from microcytic HCC cases suggest that a high degree of hepatic iron overloading could be a potential differential for unexplained microcytosis in dogs, possibly secondary to aberrant up-regulation of hepcidin. Since iron overload is associated with the onset and progression of human HCC<sup>67</sup>, and was correlated with poor histologic differentiation in our canine study, evaluation of hematologic parameters for evidence of iron-restricted erythropoiesis in dogs could be a non-invasive initial screening tool for poorly



differentiated HCC, or could provide information about clinical progression, prognosis at time of HCC diagnosis, or response to treatment. Future studies and survival analyses of dogs with microcytosis and HCC are needed to draw any definitive conclusions.

Given the increased iron loading found in the peritumoral liver tissue of our HCC cases, we expected ferritin expression to be increased in the same tissue since its primary function is to store intracellular iron. Ferritin expression levels were unremarkable between peritumoral non-HCC liver tissue and HCC tumor tissue. This may be because like ferroportin, ferritin is post-transcriptionally regulated predominantly by the iron response element (IRE)/iron regulatory protein (IRP) system<sup>68</sup>. Ferritin mRNA contains an IRE in the 5' untranslated region (UTR) to which the IRPs bind under iron deficiency and sterically inhibit translation of the ferritin protein<sup>68,69,70</sup>. Conversely an iron loaded state decreases the IRE-binding activity of IRPs and allows for the progression of ferritin protein synthesis. Whereas IRE/IRP complexes inhibit translation of ferroportin and ferritin mRNAs under iron deficient states, IRP binding stabilizes and prevents degradation of TfR1 mRNA which allows for cellular iron acquisition<sup>56,69</sup>. So when iron supply is high, the reduced IRP binding allows for ferritin mRNA translation to store excess iron but TfR1 mRNA undergoes degradation. This difference in IRE/IRP regulation may partially explain why we see differential expression of *TfR1* in our HCC cases and not the two other IRE-containing genes that encode ferroportin and ferritin. Our results do show decreased TfR1 RNA levels in the iron overloaded peritumoral liver tissue in our HCC cases, which is consistent with the described iron-dependent IRE/IRP regulation of TfR1 expression. Additional protein studies are needed to thoroughly explore post-transcriptional differences that may occur in canine HCC.

ALT is a serum biochemical marker of hepatocellular damage and we found that levels are significantly increased in the microcytic HCC group compared to the normocytic group. The cause of injury could be due to underlying liver disease or to oxidative injury secondary to hepatic iron loading. Among the microcytic HCC cases, the increased hepcidin RNA levels in the peritumoral non-HCC liver tissue paired with anemia and low serum iron is strongly suggestive of iron-restricted erythropoiesis secondary to functional iron deficiency. Moreover, we found that hepcidin RNA counts in the adjacent peritumoral liver tissue were negatively correlated to MCV and serum iron. Taken together this data suggests that the presence of microcytosis in dogs diagnosed with HCC may be attributed to elevated hepcidin levels in the peritumoral non-HCC liver tissue, and not influenced by the tumor itself like we initially hypothesized. This increase in hepcidin RNA is most likely due to increased hepatic iron stores in the non-HCC tissue, as these were positively correlated with non-HCC hepcidin RNA counts. Histopathologic review of all cases by a board-certified anatomic pathologist (PAS) excluded cases that showed patterns of inflammation suspicious for either copper or idiopathic chronic hepatitis prior to conducting the study.

Several limitations are identified in this pilot study. Our sample size was small after exclusion of many potential HCC cases due to a lack of a pre-operative CBC and our strict exclusion criteria, so we may have seen differences in other iron regulatory proteins if a larger sample size had been used. Given the retrospective nature of this study we also did not have the ability to measure certain serum iron values typically used to describe overall iron status, such as total iron binding capacity, percent saturation of transferrin, and serum ferritin. These values are most commonly used to non-invasively evaluate iron status in serum, although they do not always sensitively detect functional versus absolute iron deficiency<sup>14</sup>. Additionally, we were not

able to measure serum or urine hepcidin<sup>71</sup> and therefore could not correlate the increased hepatic hepcidin RNA levels with serum levels. We were also limited by the small amount of archived tissue available per case, so we were not able to quantify hepatic tissue iron using flame atomic absorption spectroscopy (spectrophotometry) and used Prussian Blue stain with digital analysis as a proxy. The issue of limited tissue also restricted us to evaluating the iron regulatory genes only at the RNA level. Future immunohistochemistry (IHC) studies using antibodies against ferroportin, ferritin, and BMP6 in more canine HCC liver sections and controls would be beneficial to assess target location and staining intensity differences between tumor and adjacent peritumoral tissue so that protein can be correlated with RNA findings. IHC will serve not only to quantify proteins, but also to attribute any changes in protein expression to particular cell types within the heterogeneous sections of HCC tissue (e.g. sinusoidal endothelial cells, Kupffer cells, and hepatic stellate cells, inflammatory cells, as well as both non-neoplastic and neoplastic hepatocytes)<sup>72,73</sup>.

## CHAPTER 3: EXPANDED STUDY

### EXPANDED STUDY MATERIALS AND METHODS

#### *Case selection*

Canine HCC cases (n=15), essentially normal liver (n=8), and nonspecific reactive hepatitis (NSRH), non-neoplastic liver control (n=10) specimens definitively diagnosed via surgical liver biopsy and histopathology were found through searching the electronic medical records database at the Colorado State University Veterinary Teaching Hospital. Hematologic analyses were performed using blood work values from the most recent pre-operative CBC blood work. Using similar case exclusion criteria as in the pilot study, the number of microcytic HCC cases (2 out of the total 15) that qualified was too small for statistical comparisons so further evaluation of microcytosis was not pursued in this study.

#### *Histologic evaluation of liver sections*

The histopathology for each specimen was carefully reviewed again by a single board-certified veterinary anatomic pathologist according to WSAVA criteria. Distinction between tumor and adjacent peritumoral, non-HCC liver tissue was identified for each HCC case. Normal liver tissue and HCC samples containing chronic inflammation and individual cell necrosis were excluded to avoid using samples exhibiting patterns of injury consistent with either copper-associated or primary/idiopathic chronic hepatitis since these inflammatory conditions in the dog progress to cirrhosis, which is non-existent in canine HCC<sup>2,4,74</sup>. All cases with large foci of necrosis or cirrhosis were excluded. The inflamed non-neoplastic control group consisted of samples confirmed as nonspecific reactive hepatitis (NSRH), which was determined to be the

closest histologic resemblance to the peritumoral non-HCC liver tissue present in a large portion of our HCC cases. The NSRH cases were defined as having mild to modest periportal inflammation that was usually lymphoplasmacytic but no necrotic hepatocytes. The peritumoral non-HCC liver tissue overall contained minimal periportal inflammation and minimal fibrosis attributed to compression of parenchyma adjacent to the tumor. Cases were excluded if the medical records indicated presence of additional concurrent neoplasia or inflammatory disease processes.

#### *Perl's Prussian blue staining and tissue iron estimation*

Extra paraffin embedded tissue sections for staining with Perls Prussian blue were available for 12 out of 15 HCC cases, 7 out of 8 essentially normal liver controls, and 8 out of 10 NSRH controls in the expanded set of study samples. Once again, there was not enough archived tissue available in any of the HCC FFPE blocks to pursue hepatic iron quantification via atomic absorption spectroscopy in both tumor and peritumoral tissues. Therefore, similarly to the described methodology for the pilot study, digital images of stained sections were imported into NIS Elements Software and used to estimate iron quantity based on the total percent area of positive blue staining in pixels. The difference in the analysis of this expanded set of samples was that only hepatocytes were specifically selected for iron content analyses for estimation of true hepatocellular iron stores whereas no distinction between macrophages and hepatocytes was made in the initial pilot study.

### *RNA isolation and counting*

RNA extraction from archived FFPE blocks using a commercial kit (ReliaPrep™ FFPE Total RNA Miniprep System, Promega, Madison, WI) and RNA counting using the NanoString nCounter gene expression system were performed identical to the methods described previously in the pilot study. For this study GAPDH (glyceraldehyde-3-phosphate dehydrogenase), HMBS (hydroxymethylbilane synthase), RPS18 (ribosomal protein S18), RPL32 (ribosomal protein L32), and RPL13A (ribosomal protein L13a) were used as internal controls to accurately quantify gene expression. These housekeeping genes were selected based on a literature search for studies investigating the stability of housekeeping genes specifically in canine liver tissue<sup>75,76,77</sup>. The original 9 iron regulatory genes examined in the pilot study (HAMP, TfR1, BMP6, FTH1, FPN, HFE, IL6, SFXN5, SLC25a37) were included again in this expanded study along with the addition of 80 other genes deemed either significant in human HCC or involved in iron regulation after an extensive literature search. RNA counts generated with NanoString nCounter technology were normalized using control probes and the aforementioned housekeeping genes. The means +/- 2 SD of the negative controls were subtracted from the counts obtained for each gene for background correction.

### *Study design and statistical analyses*

Paired comparisons for differential expression analyses between HCC tumor and adjacent, peritumoral tissue data were conducted with paired t-tests using the Nanostring nSolver Advanced Analysis 2.0 software. *P*-values less than 0.05 were considered to indicate a statistically significant difference. Ratios and fold-changes in log-transformed to base 2 normalized RNA counts for HCC tumor and adjacent, peritumoral non-HCC groups were

calculated, and gene data were represented as ratios and fold-change values. Overexpressed genes in the HCC tumor tissue were represented as fold-change values greater than 1, and under-expressed genes were represented as values less than -1 (Table 3). Only genes showing significant differences in expression between HCC tumor and peritumoral, non-HCC liver tissues were reported in Table 3. The complete data set for the entire expanded gene list can be found under supplemental data (Supplementary Table 1).

Analyses of multiple comparisons for estimated iron stores and RNA counts among the HCC tissue types and controls were performed using Prism 7 for Mac OS X. Unpaired groups were compared using ordinary one-way ANOVA (Figures 6-8). Transformed log-values of normalized RNA counts were used after evaluation with Anderson-Darling normality tests due to nonnormal distributions. Correction for multiple comparisons was performed by controlling the false discovery rate using the two-stage linear step-up procedure of Benjamini, Krieger and Yekutieli. The false discovery rate was set at 0.05 and RNA count comparison figures were generated using multiplicity adjusted P values.

## **EXPANDED STUDY RESULTS**

### *Differential gene expression in HCC tumor tissue versus peritumoral non-HCC liver tissue*

Analysis performed using Nanostring nSolver Advanced Analysis software revealed significant differential gene expression between HCC tumor tissue and peritumoral non-HCC liver tissue for 28 genes (Table 3). Almost one-third (10/28) of these genes encoded proteins known to be involved in iron regulation and metabolism (bolded in Table 3) and multiple genes were associated with the WNT/ $\beta$ -catenin signaling and ferroptosis pathways. The original nine iron regulatory genes examined initially in the pilot study (Table 2) were also included in this

expanded gene set and the same findings were replicated; of the original 9 genes, hepcidin and TfR1 counts were once again significantly different between HCC tumor and peritumoral non-HCC liver tissues, whereas the remaining seven iron regulatory genes again showed no significant difference in expression between tissue types (Table 3, Table S1). Hepcidin showed the most drastic fold-change of 35.2 times lower expression and TfR1 was over-expressed (about 1.6-fold) in the HCC tumor tissue compared to the adjacent, peritumoral non-HCC liver.

**Table 3.** Significant differential expression of an expanded set of genes in HCC tumor tissue compared to adjacent peritumoral liver tissue.

Gene probe	Protein	Function	Fold change*	Ratio	P-value
ABCG2	ATP binding cassette subfamily G member 2	Role in multi-drug resistance and HCC carcinogenesis	-1.4	0.71	0.0145
APC	Adenomatous polyposis coli	WNT/ $\beta$ -catenin signaling pathway suppressor	-1.3	0.78	0.0257
BIRC5	Baculoviral IAP repeat containing 5 (Survivin)	Apoptosis inhibitor; WNT/ $\beta$ -catenin pathway target gene	2.7	2.73	0.0081
CASP3	Caspase-3	Apoptosis	-2.6	0.38	0.0078
CCNB1	Cyclin B1	Cell cycle	4.3	4.26	0.0278
CCNB2	Cyclin B2	Cell cycle	2.3	2.33	0.0372
CD44	Cluster domain 44	WNT/ $\beta$ -catenin pathway target gene	-4.8	0.21	0.0008
CXCL8	C-X-C motif chemokine ligand 8	Chemokine with tumorigenic and angiogenic properties in HCC	-6.0	0.17	0.0312
CYBB	Cytochrome B-245 beta chain	Super-oxide generating enzyme	-3.4	0.29	0.0002
<b>CYBRD1</b>	<b>Cytochrome b reductase 1</b>	<b>Iron uptake</b>	<b>-2.6</b>	<b>0.38</b>	<b>0.0382</b>
E2F1	E2F transcription factor 1	Cell cycle	12.8	12.8	0.0001
GPX1	Glutathione peroxidase 1	Protection against oxidative damage	-1.6	0.65	0.0081
<b>HAMP</b>	<b>Hepcidin</b>	<b>Major regulator of liver iron homeostasis</b>	<b>-35.2</b>	<b>0.03</b>	<b>0.0012</b>



<b>HMOX1</b>	<b>Heme oxygenase 1</b>	<b>Heme catabolism</b>	<b>-2.3</b>	<b>0.43</b>	<b>0.0118</b>
KIF4A	Kinesin family member 4A	Cellular proliferation	3.6	3.56	0.0387
<b>LCN2/NGAL</b>	<b>Lipocalin 2</b>	<b>Intracellular iron sequestration</b>	<b>7.6</b>	<b>7.59</b>	<b>0.0157</b>
<b>LTF</b>	<b>Lactotransferrin</b>	<b>Iron-binding protein</b>	<b>-5.7</b>	<b>0.18</b>	<b>0.0165</b>
MAPK14	p38 MAP kinase	Cell proliferation	-1.6	0.64	0.0037
NCF2	Neutrophil cytosolic factor 2	Oxidase	-4.2	0.24	0.0196
PTEN	Phosphatase and tensin	Akt signaling pathway suppressor	-1.5	0.65	0.0021
<b>SFXN5</b>	<b>Sideroflexin 5</b>	<b>Iron transporter and storage</b>	<b>-1.6</b>	<b>0.62</b>	<b>0.0396</b>
SOD1	Superoxide dismutase 1	Oxidative stress	-1.7	0.59	0.0021
<b>STEAP2</b>	<b>STEAP family member 2</b>	<b>Metalloreductase</b>	<b>-11.6</b>	<b>0.09</b>	<b>0.0002</b>
<b>STEAP3</b>	<b>STEAP family member 3</b>	<b>Metalloreductase</b>	<b>1.8</b>	<b>1.82</b>	<b>0.0151</b>
<b>TFR2</b>	<b>Transferrin receptor 2</b>	<b>Upstream regulator of hepcidin</b>	<b>-4.4</b>	<b>0.23</b>	<b>0.0312</b>
<b>TFRC/TFR1</b>	<b>Transferrin receptor protein 1</b>	<b>Cellular iron uptake</b>	<b>1.6</b>	<b>1.61</b>	<b>0.0155</b>
TOP2A	DNA topoisomerase II alpha	DNA transcription	7.8	7.84	0.0077

Abbreviation(s): STEAP, six transmembrane epithelial antigen of the prostate.

Fold-changes and ratios of normalized, log-transformed to base 2 RNA counts for HCC tumor tissue versus peritumoral non-HCC liver tissue groups. Only genes with statistically significant ( $p$ -value < 0.05) differences determined with paired t-testing are reported in this table.

\*Overexpressed genes in HCC tumor tissue are represented as fold-change values > 1 and under-expressed genes are represented as values < -1. Bold denotation indicates function related to iron homeostasis. The complete gene list and statistics can be found under supplemental data.

#### *Gene expression and hepatic iron comparisons to normal and NSRH liver controls*

HCC tumor and peritumoral non-HCC liver RNA counts were compared to normal liver and non-neoplastic NSRH liver groups using ordinary one-way ANOVA with correction for multiple comparisons. The genes that were differentially expressed between tumoral and peritumoral groups were analyzed and select iron-related genes with statistically significant differences among multiple tissue types are shown. The genes that were under-expressed in HCC tumor tissue displayed a similar expression pattern with regards to the other tissues groups in that

RNA levels were significantly decreased in HCC tumor tissue compared to peritumoral non-HCC liver, normal liver, and non-neoplastic NSRH liver groups (Figure 6). No significant differences in RNA levels were found between peritumoral non-HCC liver and non-neoplastic NSRH control groups for any of the iron-related genes that are under-expressed in HCC tumor (Figure 6).

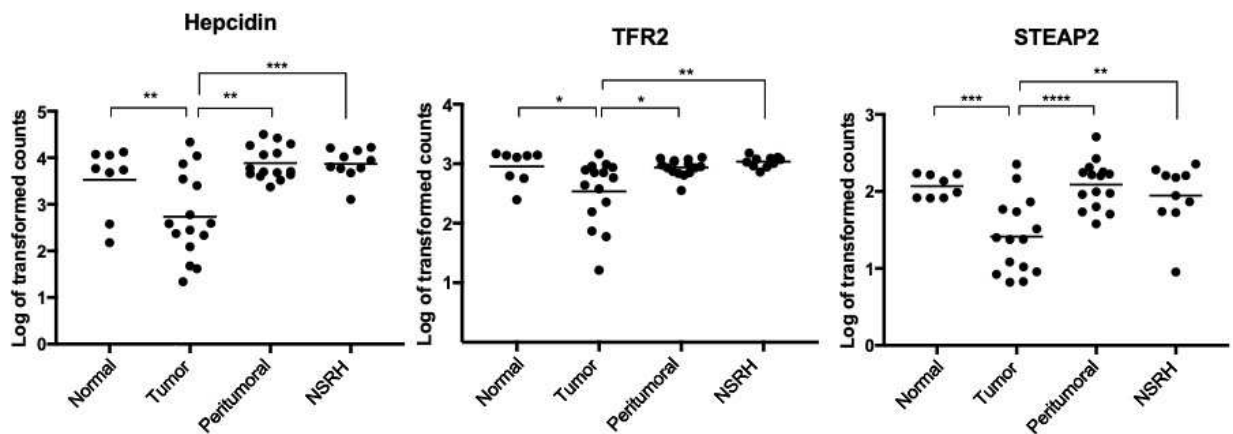


**Figure 6.** Select iron-related genes that are under-expressed in canine HCC tumor tissue. Multiple comparisons among gene expression levels in normal, HCC tumor, adjacent peritumoral, and non-neoplastic NSRH liver tissues are shown. Transformed log-values of normalized RNA counts are displayed as individual data points for each tissue group and horizontal bars represent mean values. Asterisks denote statistical significance using multiplicity adjusted P values after controlling for false discovery rate.

TfR1 and STEAP3 were the two iron-related genes over-expressed in HCC tumor tissue compared to adjacent, peritumoral non-HCC liver. Both genes display a similar expression pattern when compared to the other tissue groups in that RNA levels are increased in HCC tumor tissue but decreased in the inflamed non-neoplastic liver groups compared to peritumoral non-HCC liver and normal liver groups (Figure 7).

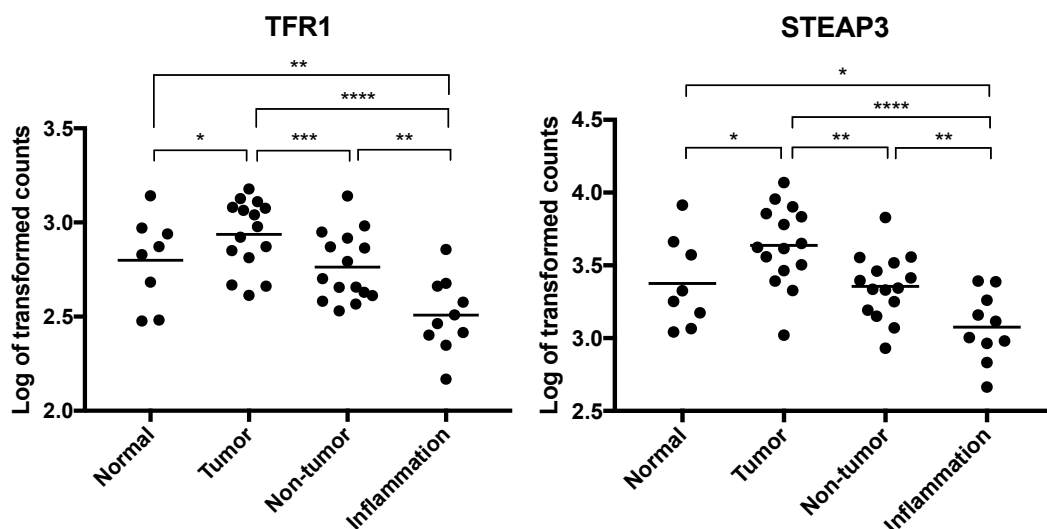


**Figure 7.** Comparisons of iron-related genes that are over-expressed in canine HCC tumor tissue to expression levels in normal, peritumoral and inflamed, non-neoplastic liver tissues. The plots show RNA counts as individual data points and their means for the indicated gene among the four tissue groups evaluated.

Hepatocellular iron stores as estimated by Perl's Prussian Blue staining were significantly increased in the adjacent peritumoral non-HCC tissue compared to HCC tumor tissue and normal liver control groups (Figure 8). No significant differences were found when peritumoral non-HCC and HCC tumor tissue iron stores were compared to those of non-neoplastic NSRH control tissues (Figure 8).

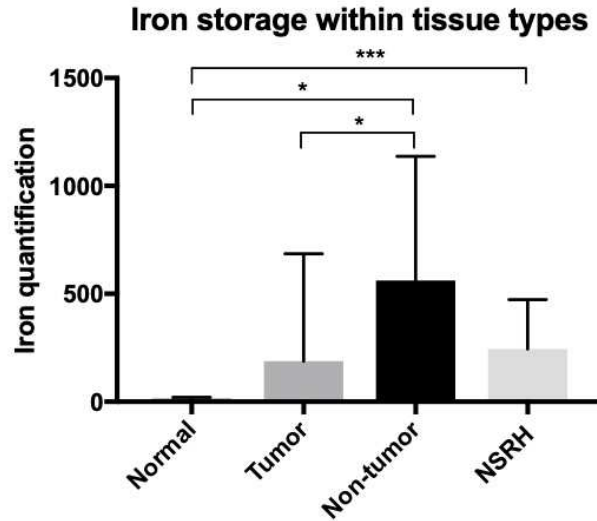


**Figure 8.** Iron quantity as estimated by digital area measurement of Perl’s Prussian Blue positive staining in hepatocytes shown for normal liver, HCC tumor, peritumoral non-HCC liver, and inflamed non-neoplastic liver tissue groups. Statistically significant differences are denoted with asterisks.

## EXPANDED STUDY DISCUSSION

A consistent major finding in both studies was that canine HCC is associated with iron loading of hepatocytes in the adjacent, peritumoral non-HCC liver tissue with a near absence of iron deposition in the actual tumor tissue itself. Although analysis of hepatic iron stores in the pilot study consisted of estimates from all liver tissue cell types (e.g. hepatocytes and Kupffer cells), the expanded study confirmed the drastic difference in intracellular iron stores to occur specifically in hepatocytes and not Kupffer cells or macrophages. This pattern of tissue iron loading was unexpected because it is well-established that neoplastic cells from a variety of cancers undergo metabolic dysregulation promoting iron accumulation in order to retain cellular supply for rapid proliferation<sup>32,78</sup>. Interestingly, this inverse pattern of iron staining has been reported in human HCC, which similarly lacks iron in tumor tissue but exhibits excessive iron deposition in adjacent non-cirrhotic, peritumoral tissue, along with a differential expression of iron regulatory genes<sup>57,59</sup>. In humans, HCC is highly associated with hepatitis B and C viral

infection or alcohol abuse which lead to the development of chronic hepatitis and cirrhosis, and eventually progression to HCC<sup>6</sup>. A previous study characterizing the histologic features of 57 HCC tumors in dogs found cirrhosis to be present in only 4 of the samples (7%), highlighting that cirrhosis is a rare concurrent condition with canine HCC<sup>1</sup>. We observed a similar absence of cirrhosis in the canine HCC tissues used in our study. The lack of an association with cirrhosis and common predisposing factors described in humans suggests a different pathogenesis for HCC in dogs.

Our study results suggest that hepatic iron overload and iron dysregulation could be contribute to HCC development in dogs. As previously mentioned, HCC develops in one-third of people diagnosed with hereditary hemochromatosis (HH)<sup>60</sup> and the relative risk for HH patients with concurrent liver cirrhosis jumps to greater than 200<sup>79</sup>, which strongly implicates excess liver iron as indirectly or synergistically contributing to the malignant transformation of hepatocytes in the face of chronic inflammation and injury in people. Much evidence in human medicine also points to excess iron potentially being directly hepatocarcinogenic in the absence of cirrhosis, though. Dietary iron overload is prevalent in sub-Saharan Africans who drink a traditional type of iron-rich beer that is home-brewed in non-galvanized steel drums, and the relative risk of subsequent HCC development is 23.5-fold in those people with the highest grade of iron accumulation despite adjustment for the confounding effect of cirrhosis<sup>61,80</sup>. Other studies have found HCC to develop in iron-loaded, non-cirrhotic livers as well<sup>81</sup> and with conditions causing secondary iron-loading such as thalassaemia<sup>82,83</sup> and myelodysplastic syndrome (MDS)<sup>84,85</sup>, both of which result in ineffective erythropoiesis and consequent excess iron deposition in the liver. Furthermore, Wistar rats fed a high-iron diet for a prolonged period developed hepatic iron overload and subsequent liver nodules which eventually progressed to HCC in the absence of

cirrhosis in one of the rats<sup>86</sup>. Histologic evaluation of HCC-containing livers from the Wistar rats, African patients with dietary iron overload, and MDS patients with secondary iron overload revealed tumors with features of moderately to well-differentiated HCC surrounded by non-cirrhotic hepatic parenchyma containing extensive iron accumulation, but minimal iron in the tumors themselves. These histologic descriptions parallel our findings in canine HCC tissues. Proliferative pre-neoplastic nodules free of iron or containing significantly less iron compared to surrounding hepatic parenchyma were also identified in iron overloaded HH patients who eventually ended up developing HCC<sup>87</sup>. The findings of these previous studies combined with our results all suggest that iron may directly induce hepatic carcinogenesis and development of canine HCC, possibly due to an unknown genetic or environmental predisposition to iron overload that could be complicated by excessive dietary iron. This possible association between iron loading and canine HCC incidence could be further investigated by conducting a larger-scale clinical follow-up study with dogs that have undergone hepatic iron quantification and determining whether there is an increased frequency of HCC in canine patients with elevated liver iron stores and if these dogs share any common genetic or environmental factors.

This second study was an extension of the pilot study to further investigate whether an abnormal iron status exists in canine HCC by examining differences in mRNA expression of iron regulatory genes in HCC tumor tissue compared to the adjacent peritumoral tissue and two control groups (normal liver and NSRH non-neoplastic liver). One of the most significant findings was that hepcidin expression was markedly reduced 35-fold in HCC tumor compared to the peritumoral non-HCC liver tissue, and when compared to normal liver and NSRH controls tumor hepcidin expression was also significantly lower. Hepcidin regulates iron by binding ferroportin and causing its degradation to prevent intracellular iron export from hepatocytes,

Kupffer cells/macrophages, and enterocytes when iron is in excess<sup>88</sup>. Our expanded study again did not find significant differences in the RNA expression levels of ferroportin as well as ferritin in canine HCC tumor and peritumoral liver tissue. We attributed this to possible post-transcriptional regulation of these genes via the IRE/IRP regulatory system in our pilot study. This expanded study included analysis of IRP1 and IRP2 mRNA, the two proteins that control cellular iron metabolism through this system, but our results did not show any significant difference in expression for these genes. The IRPs conduct their regulatory duties by binding to IRE mRNA motifs present in certain iron-related protein<sup>70</sup>, therefore analysis at the RNA level may not be representative of what is occurring post-transcriptionally.

Transferrin receptor 2 (TfR2), a potent upstream regulator of hepcidin found only in hepatocytes and erythrocytes, was also significantly under-expressed in our canine HCC tumor tissues. Normally TfR2 binds to HFE and activates the SMAD pathway to increase hepcidin expression, and studies with knockout mouse models and the liver-specific disruption TfR2 causes a significant reduction in hepcidin levels<sup>89,90</sup>. Our results show a similar concurrent reduction in both hepcidin and TfR2 expression in the HCC tumor tissue. We did not find significant expression differences in other known upstream regulators of hepcidin that we included in our expanded study such as BMP4, BMP6, BMP7 or IL-6<sup>49</sup>. BMP6 and IL6 were originally included in the pilot study which revealed the same results. Hepcidin regulation in canine HCC tumor may be occurring via a pathway other than the typical BMP/SMAD or JAK/STAT3 pathways described in normal liver iron homeostasis. Or it may be occurring through sinusoidal endothelial cells, which contribute to a small portion of the total RNA harvested from the heterogenous liver tissues. Further insight into the upstream molecular interactions between the cofactors HFE, TfR2, and HJV involved in transcription of hepcidin in

canine HCC is warranted, especially since mutations in these genes are responsible for the different subtypes of HH<sup>91</sup>. Conversely, expression of transferrin receptor protein 1 (TfR1), the receptor that binds to iron-bound transferrin allowing for iron entry into cells, and siderophore-binding lipocalin 2 (LCN2) were significantly up-regulated in canine HCC tumor tissue compared to the other tissue groups. Increased TfR1 and LCN2 expression is present in many different human cancer types and promotes neoplastic cell survival due to preferential iron uptake by the rapidly proliferating cells<sup>78,92</sup>.

This study of differential expression of iron regulatory genes in canine HCC reveals an interesting model of iron disturbance that has not been previously described in the dog, but parallels findings that have been observed in human HCC. Hepcidin is up-regulated in many human cancers with the exception of HCC, which exhibits significant down-regulation of hepcidin<sup>50,93</sup>. These authors theorized that increasing local hepcidin in all the other cancers sequesters iron in tumor cells and increases proliferative properties<sup>50</sup>. The significance of hepcidin down-regulation in HCC is more complicated to comprehend given that hepcidin produced by the liver has both systemic and local effects. One theory is that since the liver is the iron storage organ, lower tumor or “local” hepcidin levels has a paracrine effect and prevents ferroportin degradation in the local Kupffer cells, which are the main suppliers of iron, thus promoting iron availability for utilization by the surrounding neoplastic cells<sup>50</sup>. So even though the neoplastic hepatocytes are not accumulating intracellular iron like what is observed in other cancer types, they are probably benefitting from increased TfR1 and related iron protein levels as well as iron supply from neighboring Kupffer cells. The lack of iron accumulation in HCC tumor hepatocytes might even promote tumor cell survival due to evasion of ferroptosis, a cell-death pathway distinct from apoptosis, necrosis and autophagy that is dependent upon intracellular iron



accumulation for unchecked lipid peroxidation<sup>94</sup>. Interestingly, multiple markers and targets of ferroptosis (such as CYBB, GPX1, HMOX1, BIRC5 or Survivin)<sup>95</sup> show significant differential expression between tumor and adjacent peritumoral liver tissues in our canine HCC cases. Survivin is a noteworthy potent inhibitor of apoptosis and a direct target gene of the Wnt pathway<sup>96</sup> that is overexpressed in our canine HCC tumor tissue. Normally, survivin is highly expressed only during embryonic development and regains high levels of expression after malignant transformation in the majority of human cancers thus making it a promising tumor-specific marker in people<sup>96</sup> and possibly dogs.

The genes we found to be significant in canine HCC exhibit differential expression patterns similar to what has been described in human HCC with the exception of two members of the STEAP family of metalloreductases, STEAP2 and STEAP3. In normal cells, STEAP2 co-localizes with transferrin and TfR1 for cellular iron uptake and STEAP3 (also referred to as TSAP6 and nm1054 in the literature) plays a major role in intracellular reduction and utilization of iron<sup>97</sup>. More research is needed to clarify the role of STEAP proteins in carcinogenesis, but STEAP2 is found to be overexpressed in several human cancers, including HCC<sup>98</sup>. On the contrary, STEAP2 was markedly under-expressed in our canine HCC tumor tissues compared to all other groups, with expression levels reduced 11.6-fold compared to adjacent peritumoral liver. We find this paradoxical finding in canine HCC noteworthy since: (1) an extensive literature search failed to find any reports of reduced STEAP2 expression in human HCC subtypes; (2) reduced STEAP2 expression in canine HCC tumor tissue is second to hepcidin in being the most drastic fold-change observed among our significant differentially expressed iron regulatory genes; and (3) STEAP3 expression is significantly increased in canine HCC tumor tissue, which is also opposite of what has been described in human HCC and suggests possible

dysregulation of these two metalloredutases in canine HCC tumorigenesis. STEAP3 is normally found at high levels in the fetal livers of mouse embryos, as well as livers of adult mice and humans, and acts as a ferrireductase in both macrophage and hepatocyte cell-types<sup>97,99</sup>. STEAP3 expression has been found to be drastically decreased in cirrhosis-associated HCC tumors compared with the cirrhotic peritumoral tissue<sup>100</sup>, which is opposite of the increased STEAP3 expression found in our non-cirrhotic canine HCC tumors. This could support the possibility of an independent tumorigenic pathway for HCC in dogs that is separate from the initiating processes of chronic inflammation or cirrhosis described in people.

Among all the significant differentially expressed genes between canine HCC tumor and peritumoral tissues, STEAP3 and TfR1 were the only genes that also exhibited statistically significant differences between the NSRH control tissues and the adjacent peritumoral liver tissues from the HCC cases. This is noteworthy because the non-neoplastic NSRH tissues were included in the expanded study as a control group since this histologic classification most resembled the adjacent, non-HCC peritumoral liver tissue from the HCC cases. Therefore, differences between the NSRH and the peritumoral liver groups could highlight possible changes that occur during the gradual malignant transformation from non-neoplastic to pre-neoplastic and eventually neoplastic HCC in dogs. No significant difference in tissue iron estimates between the NSRH and the peritumoral liver groups was evident, but both groups were significantly more iron loaded compared to normal liver. Our results found that STEAP3 expression was lowest in the NSRH control group with significantly higher expression in the peritumoral liver tissue and overall highest expression in the HCC tumor tissue. This progressive increase of STEAP3 expression alongside the presence of iron loading in non-neoplastic NSRH controls and possibly

pre-neoplastic peritumoral liver tissues suggest that aberrant STEAP3 expression might be involved in the gradual tumorigenesis of canine HCC after initiation by excess hepatic iron.

STEAP3 knock-out mice result in a hypochromic microcytic anemia phenotype<sup>97,101</sup>, and similarly hepatocyte-specific TfR1 knockout mice<sup>56</sup> and mouse models with reduced erythroid TfR1 expression develop microcytic anemia with various degrees of hypochromasia, hypoferrremia, and systemic iron overload as well<sup>102,103</sup>. Therefore it is interesting that both TfR1 and STEAP3 exhibited lower expression levels in the adjacent peritumoral liver compared to HCC tumor in this expanded study, especially given our pilot study findings of higher peritumoral hepcidin expression and iron loading as well as hypoferrremia and anemia in canine HCC cases with concurrent microcytosis. STEAP3 was not one of the 9 iron-related genes originally included in the pilot study so its significance in microcytic cases of canine HCC is unknown at this time. It would be interesting to explore the relationship between hepcidin, STEAP3 and TfR1 and iron dysregulation in canine HCC even further given their various associations with microcytosis and abnormal iron regulation. Recent studies have described molecular associations between STEAP3 and TfR1<sup>93,99,104</sup> and evidence of a direct effect of hepatocellular iron content on hepcidin transcription through TfR1 and HFE in the BMP/SMAD signaling pathway<sup>56</sup>. Our results in combination with findings from other studies have us speculating whether the STEAP metalloredutases are involved in hepcidin dysregulation in canine HCC through upstream interactions with TfR1, TfR2, HFE, HJV in the BMP/SMAD pathway, but obviously our study does not answer this and more research is warranted.

The most frequently mutated genes in recent human HCC studies include p53 tumor suppressor encoding gene TP53, CTNNB1 (WNT pathway oncogene encoding beta-catenin), and the TERT promoter which regulates telomerase<sup>105,106</sup>. A larger scale multiplex molecular

profiling study similarly found that WNT or p53 signaling, or the telomerase promoter region are altered in 77% of HCC patients<sup>107</sup>. We did not observe a significant difference in p53 expression between canine HCC tumor and peritumoral non-HCC liver tissue, and the only p53 inhibitor that we examined was MDM2<sup>108</sup> which showed no expression difference between the two tissue types as well. Interestingly, expression of APC, a tumor suppressor in the WNT pathway which acts as a negative upstream regulator of beta-catenin, was significantly decreased in our canine HCC tissues. Despite this difference, our study did not reveal a significant difference in beta-catenin expression between HCC tumor and peritumoral tissues. Immunohistochemical staining for  $\beta$ -catenin shows that it is mainly found in the hepatocyte membrane in normal liver tissue in humans<sup>109</sup>, but in cirrhosis and HCC,  $\beta$ -catenin expression is significantly increased in the cytoplasm and nucleus compared to the membrane<sup>110</sup>. Two subgroups of aberrant  $\beta$ -catenin localization (which occurred in 33% of the examined HCC tissues) were recognized in the latter study: one with predominantly nuclear staining, which was associated with reduced fibrosis, and the other with mainly cytoplasmic staining, which correlated with increased intra-tumoral inflammation and proliferation but not fibrosis<sup>110</sup>. A small subset of HCC tumors (15.5%) lacked  $\beta$ -catenin staining and had low presence of inflammation and fibrosis<sup>110</sup>. With this described complex relationship between  $\beta$ -catenin, inflammation and fibrosis in human HCC, it would be interesting to similarly perform  $\beta$ -catenin immunohistochemical staining and examine its hepatocellular localization in our canine HCC tissues, as well as inflammatory and normal liver controls, especially since our selected HCC tissues lacked significant inflammation and fibrosis. Even though we did not see a difference in  $\beta$ -catenin mRNA levels between HCC and normal tissues in dogs, it would be interesting to see if there might be increased nuclear localization of  $\beta$ -catenin in the tumor tissue given our finding of decreased APC expression in the tumor tissue.

When  $\beta$ -catenin is able to enter the nucleus, a complex with TCF is formed promoting transcriptional activation of WNT pathway target genes that regulate cell proliferation, migration, invasion, cell cycle, and metastasis thus contributing to tumorigenesis<sup>111</sup>.

Components of the WNT pathway are frequently mutated or have copy-number alterations in human HCC genomic studies, for example one large-scale study found that about 44% of all examined HCCs had some sort of WNT signaling dysregulation<sup>107</sup>. Liver-specific biallelic inactivation of the APC gene generated liver nodules that progressed to HCC in mice<sup>112</sup> and biallelic genetic inactivation of the APC gene has been seen to contribute to the malignant transition of sporadic HCC in people<sup>113</sup>, emphasizing its importance in liver tumorigenesis. Inactivating APC mutation in colorectal cancer is a well-described early event in its carcinogenesis, and iron transport dysregulation has been described as well<sup>78</sup>. Iron loading has been found to increase WNT signaling in cultured cells, resulting in increased cell proliferation in the presence of aberrant APC or  $\beta$ -catenin<sup>114</sup>. In a mouse model with inactivated APC, high dietary iron levels compared to systemic iron accelerated intestinal tumor formation, and the authors suggested that the direct exposure of the intestinal epithelium to dietary iron may be the reason for WNT signaling modification under these conditions<sup>115</sup>. The same study found that high dietary iron levels induced TfR1 expression in intestinal polyps of these mice, as well as in human adenomas and carcinomas<sup>115</sup>. These effects of iron loading on WNT signaling is theorized to exacerbate intestinal tumorigenesis in a background of APC mutation in colorectal cancer<sup>78,114</sup>. It is possible that excess hepatic iron loading, as is seen in the adjacent non-tumor tissue in dogs, could similarly exacerbate tumorigenesis in the background of APC inactivation or aberrant WNT signaling in canine HCC as well.

We recognize that our gene expression and iron storage analyses stem from investigation of whole HCC tumor tissue, which is not specific to neoplastic hepatocytes due to the presence of multiple cell types such as sinusoidal endothelial cells, Kupffer cells (liver macrophages), hepatic stellate cells, and leukocytes. The heterogeneity of HCC is well-studied in the human literature and brings attention to diverse tumor cell subclones that occur through genetic evolution of survival-promoting oncogene and tumor suppressor alterations, as well as variations in tumor microenvironment involving stromal cells, cancer stem cells, and immune cells<sup>72,116</sup>. Different HCC tumors exhibit varying immune profiles of infiltrating immune cells when compared to each other as well as to normal liver tissue controls<sup>116</sup>. Studies in the future involving laser capture microdissection (LCM) can select and isolate neoplastic hepatocytes of interest from paraffin-embedded tissue under direct microscopic visualization for further downstream molecular analyses. Dysregulation of the epigenome also contributes to variation in tumor subclones, such as atypical DNA methylation patterns found in chronic hepatitis associated HCC in humans<sup>117</sup>, and therefore epigenetic variation is another area worthy of investigation.

## CONCLUSIONS

Our study demonstrates an iron disturbance in canine HCC that has not been previously described in the dog and closely mimics a unique pattern found in human HCC, most notably drastically decreased expression of hepcidin and increased expression of TfR1. STEAP metalloreductases, particularly STEAP2 and STEAP3, seem to have a role in aberrant iron homeostasis in canine HCC but warrants further investigation. HCC tumor tissue was

unexpectedly iron depleted whereas iron overloading occurred in the adjacent peritumoral liver tissue in the absence of cirrhosis.

We found that microcytosis was related to hepcidin expression and iron hepatocellular stores in adjacent peritumoral liver tissue, and not the HCC tumor tissue like we originally hypothesized. Microcytosis was also associated with noteworthy clinical findings such as increased ALT, lower HCT and serum iron, and histologically more poorly-differentiated tumors. Evaluation of MCV could be a useful noninvasive parameter for prognosis and clinical monitoring.

Differential expression of genes involved in Wnt signaling and ferroptosis was observed in canine HCC tumor compared to the adjacent peritumoral liver tissue. Further investigation of these pathways in canine HCC may provide new drug targets and biomarkers that could benefit future therapies and diagnostics. Similar to what has been described in human colorectal cancer, it is possible that excess iron stores directly exacerbate canine HCC tumorigenesis in the face of early driver mutations. Increasing surveillance for HCC in hepatic iron-overloaded dogs and considering chelation therapy may aid with disease prevention or management. The dog could be a promising animal model for non-cirrhotic HCC in people given the similarities in iron dysregulation. Dogs that develop HCC might have an unknown genetic predisposition to iron overload that is complicated by excess iron intake, and presence of microcytosis may indicate a more aggressive phenotype. Excess iron from dietary sources, such as raw food diets heavy in red meat or supplements, or secondary iron loading conditions should be further explored as a possible direct promoters of HCC in dogs.

## REFERENCES

1. Patnaik AK, Hurvitz AI, Lieberman PH, Johnson GF. Canine Hepatocellular Carcinoma. *Vet Pathol.* 1981;18(4):427-438.
2. Patnaik AK, Hurvitz AI, Lieberman PH. Canine Hepatic Neoplasms: A Clinicopathologic Study. *Vet Pathol.* 1980;17:553-564.
3. Liptak JM, Dernell WS, Monnet E, et al. Massive hepatocellular carcinoma in dogs: 48 cases (1992-2002). *J Am Vet Med Assoc.* 2004;225(8):1225-1230.
4. Kinsey JR, Gilson SD, Hauptman J, Mehler SJ, May LR. Factors associated with long-term survival in dogs undergoing liver lobectomy as treatment for liver tumors. *Can Vet J = La Rev Vet Can.* 2015;56(6):598-604.
5. Desai A, Sandhu S, Lai JP, Sandhu DS. Hepatocellular carcinoma in non-cirrhotic liver: A comprehensive review. *World J Hepatol.* 2019;11(1):1–18.
6. Monto A, Wright TL. The epidemiology and prevention of hepatocellular carcinoma. *Semin Oncol.* 2001;28(5):441-449.
7. Neumann, S. Comparison of blood parameters in degenerative liver disease and liver neoplasia in dogs. *Comp Clin Path.* 2004;12:206-210.
8. Neel JA, Snyder L, Grindem CB. Thrombocytosis: a retrospective study of 165 dogs. *Vet Clin Pathol.* 2012;41(2):216–222.
9. Woolcock AD, Keenan A, Cheung C, Christian JA, Moore GE. Thrombocytosis in 715 Dogs (2011–2015). *J Vet Intern Med.* 2017;31:1691–1699.
10. Evstatiev R, Bukaty A, Jimenez K, et al. Iron deficiency alters megakaryopoiesis and platelet phenotype independent of thrombopoietin. *Am J Hematol.* 2014;89(5):524-529.
11. Loo M, Beguin Y. The effect of human recombinant erythropoietin on platelet counts is strongly modulated by the adequacy of iron supply. *Blood.* 1999;93:3286–3293.
12. Matsuyama A, Takagi S, Hosoya K, et al. Impact of surgical margins on survival of 37 dogs with massive hepatocellular carcinoma. *N Z Vet J.* 2017;65:227-231.
13. Canali S, Zumbrennen-Bullough KB, Core AB, et al. Endothelial cells produce bone morphogenetic protein 6 required for iron homeostasis in mice. *Blood.* 2017;129:405-414.  
\*The citation on page 2 regarding low MCV and high RDW in people with HCC incorrectly refers to Canali et al. The correct source is: Wei TT, Tang QQ, Qin BD, et al. Elevated red blood cell distribution width is associated with liver function tests in patients with primary hepatocellular carcinoma. *Clin Hemorheol Microcirc.* 2016;64:149-155.
14. Radakovich LB, Santangelo KS, Olver CS. Reticulocyte hemoglobin content does not differentiate true from functional iron deficiency in dogs. *Vet Clin Pathol.* 2015;44:511-18.
15. Scott M, Stockham S. Erythrocytes In: Scott M, Stockham S, eds. *Fundamentals of Veterinary Clinical Pathology*, 2nd ed Ames, IA: Blackwell Publishing; 2008:107–223.
16. Iolascon A, De Falco L, Beaumont C. Molecular basis of inherited microcytic anemia due to defects in iron acquisition or heme synthesis. *Haematologica.* 2009;94:395-408.
17. De Domenico I, McVey WD, Kaplan J. Regulation of iron acquisition and storage: consequences for iron-linked disorders. *Nat Rev Mol Cell Biol.* 2008;9:72-81.
18. Meyer DJ, Harvey JW. Hematologic changes associated with serum and hepatic iron alterations in dogs with congenital portosystemic vascular anomalies. *J Vet Intern Med.* 1994;8:55-56.



19. Simpson KW, Meyer DJ, Boswood A, White RN, Maskell IE. Iron status and erythrocyte volume in dogs with congenital portosystemic vascular anomalies. *J Vet Intern Med.* 1997;11(1):14-9.
20. White RN, Burton CA, McEvoy FJ. Surgical treatment of intrahepatic portosystemic shunts in 45 dogs. *Vet Rec.* 1998;142(14):358-65.
21. Frowde PE, Gow AG, Burton CA, et al. Hepatic hepcidin gene expression in dogs with a congenital portosystemic shunt. *J Vet Intern Med.* 2014;28(4):1203-1205.
22. Bunch SE, Jordan HL, Sellon RK, Cullen JM, Smith JE. Characterization of iron status in young dogs with portosystemic shunt. *Am J Vet Res.* 1995;56(7):853-8.
23. Laflamme D, Mahaffey E, Allen S, Twedt D, Prasse K, Huber T. Microcytosis and iron status in dogs with surgically induced portosystemic shunts. *J Vet Intern Med.* 1994;8:212-216.
24. McConkey S. Clinical pathology: portosystemic shunt in a Labrador retriever. *Can Vet J.* 2000;41(3):235-237.
25. Aniołek O, Agnieszka B, Jarosińska A, Gajewski Z. Evaluation of frequency and intensity of asymptomatic anisocytosis in the Japanese dog breeds Shiba, Akita, and Hokkaido. *Acta Veterinaria Brno.* 2017;86(4):385-391.
26. Ganz T, Nemeth E. Hepcidin and iron homeostasis. *Biochim Biophys Acta - Mol Cell Res.* 2012;1823:1434-1443.
27. Ward DM, Kaplan J. Ferroportin-mediated iron transport: expression and regulation. *Biochim Biophys Acta.* 2012;1823:1426-1433.
28. Steinbicker AU, Muckenthaler MU. Out of balance-systemic iron homeostasis in iron-related disorders. *Nutrients.* 2013;5:3034-3061.
29. Drakesmith H, Nemeth E, Ganz T. Ironing out Ferroportin. *Cell Metab.* 2015;22:777-787.
30. Nicolas G, Bennoun M, Porteu A, et al. Severe iron deficiency anemia in transgenic mice expressing liver hepcidin. *Proc Natl Acad Sci USA.* 2002;99:4596-601.
31. Brissot P, Pietrangelo A, Adams PC, de Graaff B, McLaren CE, Loréal O. Haemochromatosis. *Nat Rev Dis Primers.* 2018;4:18016.
32. Torti SV, Manz DH, Paul BT, Blanchette-Farra N, Torti FM. Iron and Cancer. *Annu Rev Nutr.* 2018;38(1):97-125.
33. Hanahan D, Weinberg RA. Leading Edge Review Hallmarks of Cancer: The Next Generation. *Cell.* 2011;144:646-674.
34. Stevens RG, Graubard BI, Micozzi MS, Neriishi K, Blumberg BS. Moderate elevation of body iron level and increased risk of cancer occurrence and death. *Int. J. Cancer.* 1994;56:364-69.
35. Wu T, Sempos CT, Freudenheim JL, Muti P, Smit E. Serum iron, copper and zinc concentrations and risk of cancer mortality in US adults. *Ann. Epidemiol.* 2004;14:195-201.
36. Merk K, Mattsson B, Mattsson A, Holm G, Gullbring B, Bjorkholm M. The incidence of cancer among blood donors. *Int. J. Epidemiol.* 1990;19:505-9.
37. Hjalgrim H, Edgren G, Rostgaard K, Reilly M, Tran TN, et al. Cancer incidence in blood transfusion recipients. *J. Natl. Cancer Inst.* 2007;99:1864-74.
38. Zacharski LR, Chow BK, Howes PS, Shamayeva G, Baron JA, et al. Decreased cancer risk after iron reduction in patients with peripheral arterial disease: results from a randomized trial. *J. Natl. Cancer Inst.* 2008;100:996-1002.
39. Cross AJ, Leitzmann MF, Gail MH, Hollenbeck AR, Schatzkin A, Sinha R. A prospective study of red and processed meat intake in relation to cancer risk. *PLOS Med.* 2007;4:e325.

40. Zhu CS, Pinsky PF, Kramer BS, Prorok PC, Purdue MP, et al. The Prostate, Lung, Colorectal, and Ovarian Cancer Screening Trial and its associated research resource. *J. Natl. Cancer Inst.* 2013;105:1684–93.
41. Cross AJ, Ferrucci LM, Risch A, Graubard BI, Ward MH, et al. A large prospective study of meat consumption and colorectal cancer risk: an investigation of potential mechanisms underlying this association. *Cancer Res.* 2010;70:2406–14.
42. Alexander DD, Weed DL, Cushing CA, Lowe KA. Meta-analysis of prospective studies of red meat consumption and colorectal cancer. *Eur. J. Cancer Prev.* 2011;20:293–307.
43. Carr PR, Walter V, Brenner H, Hoffmeister M. Meat subtypes and their association with colorectal cancer: systematic review and meta-analysis. *Int. J. Cancer.* 2016;138:293–302.
44. Pietrangelo A. Genetics, Genetic Testing, and Management of Hemochromatosis: 15 Years Since HfeC1. *Gastroenterology.* 2015;149(5):1240-1251.e4.
45. Corradini E, Meynard D, Wu Q. Serum and liver iron differently regulate the bone morphogenetic protein 6 (BMP6)-SMAD signaling pathway in mice. *Hepatology.* 2011; 54:273-284.
46. Elmberg M, Hultcrantz R, Ekbom A, et al. Cancer risk in patients with hereditary hemochromatosis and in their first-degree relatives. *Gastroenterology.* 2003;125(6):1733-1741.
47. Fargion S, Valenti L, Fracanzani AL. Hemochromatosis gene (HFE) mutations and cancer risk: Expanding the clinical manifestations of hereditary iron overload. *Hepatology.* 2010;51(4):1119-1121.
48. Pusatcioglu CK, Nemeth E, Fantuzzi G, Llor X, Freels S, Tussing-Humphreys L et al. Systemic and tumor level iron regulation in men with colorectal cancer: a case control study. *Nutr Metab.* 2014;11:21.
49. Tesfay L, Clausen KA, Kim JW, Hegde P, Wang X, Miller LD et al. HfeC1 regulation in prostate and its disruption in prostate cancer. *Cancer Res.* 2015; 75:2254–2263.
50. Vela D, Vela-Gaxha Z. Differential regulation of hepcidin in cancer and non-cancer tissues and its clinical implications. *Exp Mol Med.* 2018;50:e436.
51. Bogdan AR, Miyazawa M, Hashimoto K, Tsuji Y. Regulators of Iron Homeostasis: New Players in Metabolism, Cell Death, and Disease. *Trends in Biochemical Sciences.* 2016;41:274-286.
52. Sprague WS, Hackett TB, Johnson JS, Swardson-Olver CJ. Hemochromatosis secondary to repeated blood transfusions in a dog. *Vet Pathol.* 2003;40:334-337.
53. Tsang HF, Xue VW, Koh SP, Chiu YM, Ng LPW, Wong SCC. NanoString, a novel digital color-coded barcode technology: current and future applications in molecular diagnostics. *Expert Rev Mol Diagn.* 2017;17:95-103.
54. Geiss GK, Bumgarner RE, Birditt B, et al. Direct multiplexed measurement of gene expression with color-coded probe pairs. *Nat Biotechnol.* 2008;26:317-325.
55. Nemeth E. Iron regulation and erythropoiesis. *Curr Opin Hematol.* 2008;15:169-75.
56. Fillebeen C, Charlebois E, Wagner J, Katsarou A, Mui J, Vali H, Garcia-Santos D, Ponka P, Presley J, Pantopoulos K. Transferrin receptor 1 controls systemic iron homeostasis by fine-tuning hepcidin expression to hepatocellular iron load. *Blood.* 2019;133(4):344–355.
57. Tseng HH, Chang JG, Hwang YH, Yeh KT, Chen YL, Yu HS. Expression of hepcidin and other iron-regulatory genes in human hepatocellular carcinoma and its clinical implications. *J Cancer Res Clin Oncol.* 2009;135:1413-1420.

58. Muckenthaler MU, Rivella S, Hentze MW, Galy B. Review A Red Carpet for Iron Metabolism. *Cell*. 2017;3:1-18.
59. Tan MG, Kumarasinghe MP, Wang SM, Ooi LL, Aw SE, Hui KM. Modulation of iron-regulatory genes in human hepatocellular carcinoma and its physiological consequences. *Exp Biol Med*. 2009;234:693-702.
60. Niederau C, Fischer R, Sonnenberg A, Stremmel W, Trampisch HJ, Strohmeyer G. Survival and Causes of Death in Cirrhotic and in Noncirrhotic Patients with Primary Hemochromatosis. *N Engl J Med*. 1985;313:1256-62.
61. Gordeuk VR, McLaren CE, MacPhail AP, Deichsel G, Bothwell TH. Associations of iron overload in Africa with hepatocellular carcinoma and tuberculosis: Strachan's 1929 thesis revisited. *Blood*. 1996;87:3470-3476.
62. Kowdley KV. Iron overload in patients with chronic liver disease. *Gastroenterol Hepatol*. 2016;12:695-698.
63. Ma S, Yang J, Li J, Song J. The clinical utility of the proliferating cell nuclear antigen expression in patients with hepatocellular carcinoma. *Tumor Biol*. 2016;37:7405-7412.
64. Schultheiss PC, Bedwell CL, Hamar DW, Fettman MJ. Canine liver iron, copper, and zinc concentrations and association with histologic lesions. *J Vet Diagn Invest*. 2002;14:396-402.
65. Harro CC, Smedley RC, Buchweitz JP, Langlois DK. Hepatic copper and other trace mineral concentrations in dogs with hepatocellular carcinoma. *J Vet Intern Med*. 2019;33:2193-2199.
66. Johnson CA, Armstrong PJ, Hauptman JG. Congenital portosystemic shunts in dogs: 46 cases (1979-1986). *J Am Vet Med Assoc*. 1987;191:1478-1483.
67. Deugnier Y, Turlin B. Pathology of hepatic iron overload. *Semin Liver Dis*. 2011;13:4755-4760.
68. Anderson ER, Shah YM. Iron homeostasis in the liver. *Compr Physiol*. 2013;3(1):315-330.
69. Wang J, Pantopoulos K. Regulation of cellular iron metabolism. *Biochem J*. 2011;434(3):365-381.
70. Muckenthaler MU, Galy B, Hentze MW. Systemic iron homeostasis and the iron-responsive element/iron-regulatory protein (IRE/IRP) regulatory network. *Annual review of nutrition*. 2008;28:197-213.
71. Vizi Z, Lányi K, Bagi M, Laczay P, Balogh N, Sterczar Á. Serum hepcidin measurements in healthy dogs using liquid chromatography/tandem mass spectrometry. *Vet Clin Pathol*. 2020;49:292-298.
72. Liu J, Dang H, Wang XW. The significance of intertumor and intratumor heterogeneity in liver cancer. *Exp Mol Med*. 2018; e416. doi:10.1038/emm.2017.165
73. Zhang S, Chang W, Wu H, et al. Pan-cancer analysis of iron metabolic landscape across the Cancer Genome Atlas. *J Cell Physiol*. 2020;235:1013-1024.
74. Webster et al. ACVIM consensus statement on the diagnosis and treatment of chronic hepatitis in dogs. *J Vet Intern Med*. 2019;33:1173-1200.
75. Lejnine S, Marton MJ, Wang IM, Howell BJ, Webber AL, Maxwell JW, Shire N, Malkov V, Lunceford J, Zeremski M, Sun A, Ruddy M, Talal AH. Gene expression analysis in serial liver fine needle aspirates. *J Viral Hepat*. 2015;22(1):64-76.
76. Peters IR, Peeters D, Helps CR, Day MJ. Development and application of multiple internal reference (housekeeper) gene assays for accurate normalisation of canine gene expression studies. *Vet Immunol Immunopathol*. 2007;15;117(1-2):55-66.

77. Brinkhof B, Spee B, Rothuizen J, Penning LC. Development and evaluation of canine reference genes for accurate quantification of gene expression. *Anal Biochem.* 2006;1;356(1):36-43.
78. Torti SV, Torti FM. Iron and cancer: More ore to be mined. *Nat Rev Cancer.* 2013;13:342-55.
79. Bradbear RA, Bain C, Siskind V et al. Cohort study of internal malignancy in genetic hemochromatosis and other chronic non-alcoholic liver disease. *J. Natl Cancer Inst.* 1985;75:81-4.
80. Kew MC, Asare GA. Dietary iron overload in the African and hepatocellular carcinoma. *Liver International.* 2007;27:735-741.
81. Turlin B, Juguet F, Moirand R, Le Quilleuc D, Loreal O, Champion JP, Launois B, et al. Increased liver iron stores in patients with hepatocellular carcinoma developed on a noncirrhotic liver. *Hepatology.* 1995;22(2):446-450.
82. Moukhadder HM, Halawi R, Cappellini MD, Taher AT. Hepatocellular carcinoma as an emerging morbidity in the thalassemia syndromes: A comprehensive review. *Cancer.* 2017;123:751-758.
83. Borgna-Pignatti C, Vergine G, Lombardo T, et al. Hepatocellular carcinoma in the thalassaemia syndromes. *Br J Haematol.* 2004;124:114-7.
84. Ikoma N, Shinozaki H, Kozuki A, et al. A case report of hepatocellular carcinoma in a non-cirrhotic patient with liver iron overload associated with myelodysplastic syndrome. *World J Oncol.* 2013;4:248-251.
85. Yamauchi R, Takata K, Shinagawa Y, et al. Hepatocellular Carcinoma Arising in a Non-cirrhotic Liver with Secondary Hemochromatosis. *Intern Med.* 2019;58(5):661-665.
86. Asare GA, Paterson AC, Kew MC, Khan S, Mossanda KS. Iron-free neoplastic nodules and hepatocellular carcinoma without cirrhosis in Wistar rats fed a diet high in iron. *J. Pathol.* 2006;208:82-90.
87. Deugnier YM, Charalambous P, Le Quilleuc D et al. Preneoplastic significance of hepatic iron-free foci in genetic hemochromatosis: a study of 185 patients. *Hepatology.* 1993;18:1363-9.
88. Rishi G, Wallace D, and Subramaniam V. Hcpidin: regulation of the master iron regulator. *Biosciences Reports.* 2015;35(3):e00192.
89. Kawabata H, Fleming RE, Gui D, Moon SY, Saitoh T, O'Kelly J, Umehara Y, Wano Y, Said JW, Koeffler HP. Expression of hepcidin is down-regulated in TfR2 mutant mice manifesting a phenotype of hereditary hemochromatosis. *Blood.* 2005;105(1):376-81.
90. Wallace DF, Summerville L, Subramaniam VN. Targeted disruption of the hepatic transferrin receptor 2 gene in mice leads to iron overload. *Gastroenterology.* 2007;132(1):301-10.
91. Lee PL, Beutler E. Regulation of hepcidin and iron-overload disease. *Annu. Rev. Pathol.* 2009;4:489-515.
92. Xiao X, Yeoh BS, Vijay-Kumar M. Lipocalin 2: An Emerging Player in Iron Homeostasis and Inflammation. *Annu. Rev. of Nutrition.* 2017;37(1):103-130.
93. Zhang S, Chang W, Wu H, et al. Pan-cancer analysis of iron metabolic landscape across the Cancer Genome Atlas. *J Cell Physiol.* 2019;235:1013-1024.
94. Dixon SJ, Lemberg KM, Lamprecht MR, et al. Ferroptosis: an iron-dependent form of nonapoptotic cell death. *Cell.* 2012;149(5):1060-1072.

95. Zhou N, Bao J. FerrDb: a manually curated resource for regulators and markers of ferroptosis and ferroptosis-disease associations. *Database*. 2020;2020: article ID baaa021; doi:10.1093/database/baaa021
96. Su C. Survivin in survival of hepatocellular carcinoma. *Cancer Letters*. 379(2);2016:184-190.
97. Ohgami RS, Campagna DR, Antiochos B, Wood EB, Sharp JJ, Barker JE, et al. nm1054: a spontaneous, recessive, hypochromic, microcytic anemia mutation in the mouse. *Blood*. 2005;106:3625–31.
98. Gomes IM, Maia CJ, Santos CR. STEAP Proteins: From Structure to Applications in Cancer Therapy. *Mol Cancer Res*. 2012;10(5):573-587.
99. Zhang F, Tao Y, Zhang Z, et al. Metalloreductase Steap3 coordinates the regulation of iron homeostasis and inflammatory responses. *Haematologica*. 2012;97(12):1826–1835.
100. Caillot F, Daveau R, Daveau M, Lubrano J, Saint-Auret G, Hiron M, et al. Down-regulated expression of the TSAP6 protein in liver is associated with a transition from cirrhosis to hepatocellular carcinoma. *Histopathology*. 2009;54:319–27.
101. Blanc L, Papoin J, Debnath G, Vidal M, Amson R, Telerman A, An X, Mohandas N. Abnormal erythroid maturation leads to microcytic anemia in the TSAP6/Steap3 null mouse model. *Am. J. Hematol*. 2015;90:235-241.
102. Zhu BM, McLaughlin SK, Na R, et al. Hematopoietic-specific Stat5-null mice display microcytic hypochromic anemia associated with reduced transferrin receptor gene expression. *Blood*. 2008;112(5):2071-2080.
103. Cooperman SS, Meyron-Holtz EG, Olivierre- Wilson H, Ghosh MC, McConnell JP, Rouault TA. Microcytic anemia, erythropoietic proto- porphyria, and neurodegeneration in mice with targeted deletion of iron-regulatory protein 2. *Blood*. 2005;106(3):1084-1091.
104. Jabara H, Boyden S, Chou J, et al. A missense mutation in TFRC, encoding transferrin receptor 1, causes combined immunodeficiency. *Nat Genet*. 2016;48:74–78.
105. Schulze K, Imbeaud S, Letouzé E, et al. Exome sequencing of hepatocellular carcinomas identifies new mutational signatures and potential therapeutic targets. *Nat Genet*. 2015;47:505–511.
106. Totoki Y, Tatsuno K, Covington K, et al. Trans-ancestry mutational landscape of hepatocellular carcinoma genomes. *Nat Genet*. 2014;46:1267–1273.
107. Cancer Genome Atlas Research Network. Electronic address: wheeler@bcm.edu; Cancer Genome Atlas Research Network. Comprehensive and Integrative Genomic Characterization of Hepatocellular Carcinoma. *Cell*. 2017;169(7):1327–1341.e23
108. Eischen CM, Lozano G. The Mdm network and its regulation of p53 activities: a rheostat of cancer risk. *Hum Mutat*. 2014;35(6):728–737.
109. Li P, Cao Y, Li Y, Zhou L, Liu X, Geng M. Expression of Wnt-5a and B-catenin in primary hepatocellular carcinoma. *Int J Clin Exp Pathol*. 2014;7(6):3190–3195.
110. Lee JM, Yang J, Newell P, et al.  $\beta$ -Catenin signaling in hepatocellular cancer: implications in inflammation, fibrosis, and proliferation. *Cancer Lett*. 2014;343(1):90–97.
111. Waisberg J, Saba GT. Wnt-/- $\beta$ -catenin pathway signaling in human hepatocellular carcinoma. *World J Hepatol*. 2015;7(26):2631–2635.
112. Colnot S, Decaens T, Niwa-Kawakita M, Godard C, Hamard G, Kahn A, Giovannini M, Perret C. Liver-targeted disruption of Apc in mice activates b-catenin signaling and leads to hepatocellular carcinomas. *Proc Natl Acad Sci*. 2004;101:17216–17221.

113. Katoh H, Shibata T, Kokubu A, Ojima H, Kosuge T, Kanai Y, Hirohashi S. Genetic inactivation of the APC gene contributes to the malignant progression of sporadic hepatocellular carcinoma: A case report. *Genes Chromosom. Cancer*. 2006;45:1050-1057.
114. Brookes MJ, et al. A role for iron in Wnt signalling. *Oncogene*. 2008;27:966–975.
115. Radulescu S, et al. Luminal iron levels govern intestinal tumorigenesis after Apc loss in vivo. *Cell Rep*. 2012;2:270–282.
116. Zhang Q, Lou Y, Yang J, et al. Integrated multiomic analysis reveals comprehensive tumour heterogeneity and novel immunophenotypic classification in hepatocellular carcinomas. *Gut*. 2019;68:2019–2031.
117. Kondo Y, Kanai Y, Sakamoto M, Mizokami M, Ueda R, Hirohashi S. Genetic instability and aberrant DNA methylation in chronic hepatitis and cirrhosis—A comprehensive study of loss of heterozygosity and microsatellite instability at 39 loci and DNA hypermethylation on 8 CpG islands in microdissected specimens from patients with hepatocellular carcinoma. *Hepatology*. 2000;32:970–979.

## APPENDICES

### SUPPLEMENTAL DATA

**Table S1.** Complete differential expression data for genes (n=89) examined in the expanded study known to be involved in iron homeostasis or human hepatocellular carcinoma pathogenesis. Comparisons performed as HCC tumor tissue versus peritumoral, non-HCC liver tissue.

<b>Gene probe</b>	<b>Fold change*</b>	<b>Ratio</b>	<b>P-value</b>
ABCG2	-1.4	0.71	0.0145
ACVR1	-1.04	0.97	0.8316
ADAM10	-1.11	0.9	0.5540
AKT	-1.13	0.89	0.4078
ALAD	-1.24	0.81	0.2597
ALAS1	-1.21	0.83	0.5344
ALAS2	-2.46	0.41	0.0941
APC	-1.29	0.78	0.0257
AXIN2	-2.51	0.4	0.2523
BAX	1.16	1.16	0.7350
BCL2	1.79	1.79	0.2333
BIRC5	2.73	2.73	0.0081
BMP4	-1.88	0.53	0.0683
BMP6	1.55	1.55	0.1931
BMP7	3.02	3.02	0.1144
CASP3	-2.62	0.38	0.0078
CCNB1	4.26	4.26	0.0277
CCNB2	2.33	2.33	0.0372
CD25	1.33	1.33	0.4186
CD44	-4.78	0.21	0.0008
CDK4	1.12	1.12	0.3979
CDKN1A	1.53	1.53	0.3759
CDKN1B	1.12	1.12	0.6747
CDKN2a	-1	1	0.9997
CDKN2b	2.49	2.49	0.1562
CP	-1.28	0.78	0.1428
CSNK1A1	1.01	1.01	0.9758
CTNNB1	1.04	1.04	0.8540
CXCL8	-5.96	0.17	0.0312
CYBB	-3.4	0.29	0.0002

CYBRD1	-2.61	0.38	0.0382
E2F1	12.82	12.82	0.0001
EPAS1	-1.07	0.94	0.7911
FECH	-1.06	0.94	0.7313
FLVCR1	-1.75	0.57	0.2073
FTH1	-1.22	0.82	0.0506
FXN	-1.22	0.82	0.1660
FOSL1	1.03	1.03	0.9606
GLRX5	1.3	1.3	0.2717
GPX1	-1.55	0.65	0.0081
GSK3B	1.02	1.02	0.7639
HAMP	-35.17	0.03	0.0012
HEPH	1.24	1.24	0.4316
HFE	-1.2	0.83	0.6041
HFE2	-1.12	0.89	0.6403
HIF1A	-1.1	0.91	0.6627
HIF1AN	1.3	1.3	0.3074
HMOX1	-2.33	0.43	0.0118
HRAS	-1.15	0.87	0.4825
IL6	1.43	1.43	0.3828
IRP1	-1.38	0.72	0.0734
IRP2	1.2	1.2	0.2271
ISCU	-1.32	0.76	0.0688
JUN	-1.12	0.89	0.7737
KIF4A	3.56	3.56	0.0387
LCN2/NGAL	7.59	7.59	0.0157
LTF	-5.71	0.18	0.0165
MAPK14	-1.56	0.64	0.0037
MAPK8	-1.97	0.51	0.1823
MDM2	1.18	1.18	0.3636
MET	1.07	1.07	0.6137
MMP2	-1.03	0.97	0.9643
MYC	-1.01	0.99	0.9687
NCF2	-4.21	0.24	0.0196
NDRG1	-1.42	0.7	0.4914
PTEN	-1.53	0.65	0.0021
PTPRZ1	1.16	1.16	0.5940
SCARA5	1.84	1.84	0.1190
SFXN1	1.1	1.1	0.6058
SFXN5	-1.61	0.62	0.0396



SLC11A2	-1.06	0.94	0.8200
SLC22A17	-2.29	0.44	0.1707
SLC25A37	-1.58	0.63	0.2185
SLC40A1	-1.29	0.78	0.3116
SLC7A1	1.06	1.06	0.8995
SOD1	-1.69	0.59	0.0021
SRF	-1.1	0.91	0.7770
STAT3	1.02	1.02	0.9033
STEAP1	-1.01	0.99	0.9683
STEAP2	-11.6	0.09	0.0002
STEAP3	1.82	1.82	0.0151
TF	-1.44	0.7	0.1814
TFR2	-4.41	0.23	0.0312
TFRC	1.61	1.61	0.0155
TMPRSS6	-2.55	0.39	0.0762
TNF	-2.74	0.36	0.0737
TOP2A	7.84	7.84	0.0077
TP53	1.06	1.06	0.7792
TP73	1.4	1.4	0.2392

\*Fold-changes in normalized, log-transformed to base 2 RNA counts for HCC tumor tissues versus peritumoral non-HCC liver tissues. *P*-values were determined with paired t-testing. Overexpressed genes being represented as values > 1 and under-expressed genes being represented as values <-1.